Università
Ca'Foscari
Venezia

Master's Degree

in science and technology of bio and nanomaterials

Final Thesis

Synthesis and characterization of polyethylene glycol-coated hierarchical ferrite nanoparticles as contrast agents for magnetic resonance imaging applications

Supervisor
Prof. Flavio Rizzolio

Co supervisor
Dr. Ghasem Dini

Graduand
Sedigheh Cheraghali
882462

Academic Year
2022 / 2023

Abstract

Ferrite nanoparticles containing manganese and zinc have numerous applications in medicine, especially in magnetic resonance imaging (MRI) as contrast agents to improve the quality of MRI images. In recent decades, magnetic resonance imaging (MRI) has become an established diagnostic tool for in vivo anatomical imaging. MRI has also become one of the most powerful diagnostic methods in biomedical imaging. However, the toxic and destructive effects of using contrast agents on the body should be considered. These nanoparticles, known as MRI contrast agents, should have a high magnetic property, a particle size of less than 100 nm, and a narrow size distribution. In addition, a hierarchical structure was achieved by adding ascorbic acid and urea, which increased the specific surface area of the nanoparticles. Furthermore, the nanoparticles need to be coated with suitable polymers to reduce toxicity and increase their biocompatibility.

Therefore, in this study, hierarchical Mn-Zn ferrite nanoparticles were synthesized using ferric chloride, zinc chloride, manganese chloride, ascorbic acid, and urea via the hydrothermal method at a temperature of 160 °C and a process time of 6 hours. The resulting precipitates were then dried at 70˚C for 10 hours, followed by annealing at 500 C for 2 hours. The pH was measured in three different steps: first by adding 3 salts (pH = 1.7), then by adding ascorbic acid (pH = 1.12), and finally by adding urea (pH = 1.30). The nanoparticles were coated with biodegradable coatings of the polymer polyethylene glycol (PEG) to improve the dispersibility, biocompatibility, and stability of the manganese-zinc-ferrite nanoparticles.

The crystal structure, chemical composition, morphology, and mean particle size of the synthesis were determined by XRD, SEM, ICP-mass, and DLS analysis. The presence of a PEG coating on the surface of the nanoparticles was investigated by TEM and FTIR analysis. VSM analysis was used to study the magnetic properties of the synthesized and coated nanoparticles. To verify the blood compatibility of the hierarchical Mn-Zn nanoparticles, complete blood count (CBC) and in vitro blood coagulation studies were also performed. Finally, we used an in vitro MRI assay to verify the image resolution of these ferrite nanoparticles.

Keywords: Mn-Zn Ferrite Nanoparticles, Hydrothermal, Hierarchical, Magnetic Properties, Biocompatibility, Contrast Factors, Magnetic Resonance Imaging (MRI)

Table of Contents

Table of figures

Table of tables

Chapter 1

Introduction

In the last two decades, magnetic nanoparticles (NPs) have triggered many research activities due to their increasing application in biological and medical systems, as well as their interesting structures and expected multifunctional and advanced applications in magnetic fluid hyperthermia, medical imaging diagnosis, and targeted drug delivery. (PHAM THANH PHONG, 2015). The synthesis of superparamagnetic nanoparticles has been greatly expanded not only because of their considerable scientific utility but also because of their numerous technological uses: including magnetic storage media, biosensor applications, medical applications such as targeted drug delivery, contrast agents for magnetic resonance imaging (MRI), etc. The control of monodisperse size is very important because the properties of nanocrystals strongly depend on the size of nanoparticles. (Sophie Laurent, 2008)

To increase the signal and image contrast, it is very important to decrease the reduction time of T_1 and T_2. The materials most commonly used in MRI are paramagnetic compounds such as gadolinium, a heavy metal and component of the lanthanides, which is highly toxic in its free state. Compared to conventional paramagnetic MRI contrast agents based on gadolinium compounds, iron oxide nanoparticles exhibit excellent magnetization and longer circulation times because gadolinium ions rapidly leave the circulatory system and are excreted via the kidneys or liver, giving them only a brief opportunity to disperse. (Jessica Wahsner, 2018)

Accurate studies of fluid stability, particle sizes, materials, physical behavior, and surfactant control are needed to identify the behavior of ferrofluids and to modify

applications or develop new ones. (Oscar Oehlsen, 2022) It is also important that the nanoparticles are narrow, small, and coated with a suitable polymer to improve stability and biocompatibility. Superparamagnetic iron oxide nanoparticles with suitable surface chemistry can be used for numerous in vivo applications, such as tissue repair, MRI contrast enhancement, immunoassay, detoxification of biological fluids, cell separation, hyperthermia, and drug delivery.

MRI contrast agents are also injected intravenously and distributed throughout the body. Relatively high doses of gadolinium per kilogram of body weight indicate that the complexes should remain inactive in the body, but gadolinium ions are toxic. Because of their size and electrical charge, which resemble elements such as zinc or calcium, they can be replaced by them and cause excretion of these elements through the urine and dysfunction of the body. (FDA Drug Safety Communication: FDA warns that gadolinium-based contrast agents (GBCAs) are retained in the body; requires new class warnings, 2017). People with acute liver disease are at increased risk for disability and fatal disease.

Therefore, many efforts have been made in recent years to develop new contrast agents. One of them is magnetic nanoparticles, which are used as contrast agents in MRI. For many clinical applications, the magnetic properties of magnetite, such as its saturation magnet, need to be improved. One way to improve the magnetic properties of Fe_3O_4 is to add elements such as manganese, zinc, cobalt etc. to the magnetic structure. (Bashar Issa, 2013)

Magnetic nanoparticles have been synthesized in various ways, including physical and chemical methods. So far, many researches have been carried out on the synthesis of $MnFe_2O_4$ ferrite nanoparticles by hydrothermal processes (Thomas Dippong, 2021), but in none of them the presence of Zn and its effects on saturation magnetization as well as

hierarchical structure and effects on MRI contrast have been studied. Therefore, in this research, by using the hydrothermal method and controlling the initial production conditions such as temperature, pressure and pH, ferrite nanoparticles are prepared on Mn and Zn and then coated to improve the biocompatibility of the nanoparticles with biocompatible polymer material.

The beginning of the development of nanotechnology is not known. It can be said that medieval glassmakers used this technology for the first time. At that time gold nanoparticles were used to make the glass of some churches, and with this method they made glass with attractive colors. The term Nano was first used in 1974 by Norio Taniguchi, a professor at Tokyo College of Science. (Vishnu D.Rajput, 2021). Afterwards, American physicist Richard Feynman said in a speech the historic phrase "All of Britain can be written on a pin." Other scientists such as Heinrich Rohrer (1981) and Richard Smalley, Carroll (1985), also contributed to the development of this technology.

One of the types of nanomaterials are magnetic nanoparticles, in which the ratio of surface area-to-volume increases due to the reduction of particle size and some properties (physical, chemical, electrical, magnetic, etc.) change. (IbrahimKhan, 2019). Magnetic nanoparticles are widely used in fields such as magnetic recording, ferrofluids (a magnetic solution that becomes magnetized in the presence of a field), food industry, targeted drug delivery, and also magnetic resonance imaging (MRI).

Currently, MRI is one of the most powerful diagnostic tools in medicine, capable of imaging soft tissue with high resolution and detecting damage early. However, in most cases, the relaxation time of healthy and damaged tissue is slightly different, so the image obtained is not very accurate. (RadilogyInfo.org, 2020).In such cases, MRI contrast agents

may be used. These factors increase image resolution. Like gadolinium, it becomes one of the contrast agents. Since it is toxic alone, it is mixed with diethylenetriaminepentaacetic acid, a combination of metals and an organic ligand that reduces toxicity. On the other hand, gadolinium ions quickly leave the bloodstream and are excreted by the kidneys or liver. For this reason, there is little time for imaging. Gadolinium also has a short latency and weak signal intensity. (Michael A. Ibrahim, 2022)

Spinel ferrites with the formula MFe_2O_4 are now widely used in medical applications due to their magnetic, structural, and biological properties. (S.A.V. Prasad, 2018) For example, manganese zinc ferrite nanoparticles with the formula $Mn_aZn_{(1-a)}Fe_2O_4$ have a strong effect on MRI contrast.

Since the aim of this research is the synthesis of hierarchical manganese-zinc-ferrite nanoparticles by hydrothermal method and their coating with biocompatible organic coatings, several methods for the synthesis of magnetic nanoparticles and the study of the magnetic properties of these ferrites have been described in this chapter. By presenting the suitable polymer for coating, the medical applications of these nanoparticles, including their use in MRI, were then discussed.

Nanomaterials

Nanomaterials are materials that have a size of less than 100 nm in at least one dimension. Nanomaterials are divided into three general categories as follows: (Phi4tech, n.d.)

1- Zero-dimensional nanomaterials: when all three dimensions of the nanomaterial are in the nanometer range (such as nanoparticles). (Phi4tech, n.d.)

2- One-dimensional nanomaterials: when two dimensions of the nanomaterial are in the nanometer range (such as nanowires and carbon nanotubes). (Phi4tech, n.d.)

3- Carbon nanomaterials: when only one of the dimensions of the nanomaterial is in the nanometer range (e.g., thin coatings). (Phi4tech, n.d.)

Magnetic nanoparticles are one of the types of nanomaterials that have received much attention in recent decades due to their numerous applications in the medical industry. (P. Majewski, 2009) These nanoparticles can be synthesized in different ways. Since the size, distribution, purity, magnetic properties and morphology of nanoparticles, and thus their applications, depend on the method of preparation, the synthesis method of these materials is very important and will be briefly discussed below.

Methods for the production of nanoparticles:

In general, there are two ways to produce nanoparticles:

Top-down method:

In this approach, a bulk material is formed and modified to produce the product. In this method, a large material is taken and by reducing its dimensions and shaping it, a product with Nano dimensions is achieved. (AZO NANO, 2004) One of the most important of these methods is mechanical grinding. Mechanical grinding is usually performed under a neutral gas atmosphere and in a high-energy ball mill. The powders in the mill are constantly struck by high-energy balls, which causes the powders to repeatedly break and erode. With continued milling, this process of breaking and seizing continues, resulting in a reduction in the size of the nanoparticles. (RoshaidaArbain, 2011)

Careful monitoring of the process leads to the production of nanoparticles with desired properties. Effective parameters in this process include the type of mill (high energy or low energy mill), the materials used for the mill parts (ceramic, stainless steel, tungsten carbide). The type of grinding device (rod or ball mill), the grinding atmosphere (air, nitrogen, etc.), the grinding environment (dry or wet), the temperature, and the grinding time.

Long grinding time can bring many disadvantages to the powder obtained, for example, the possibility of balls being ground and impurities entering the powder is one of the disadvantages of long grinding time. (Saikat Chaudhuri, 2021) In addition, the size range of the particles obtained by grinding is usually very large. Figure 1 shows overview of the mechanical milling machine.

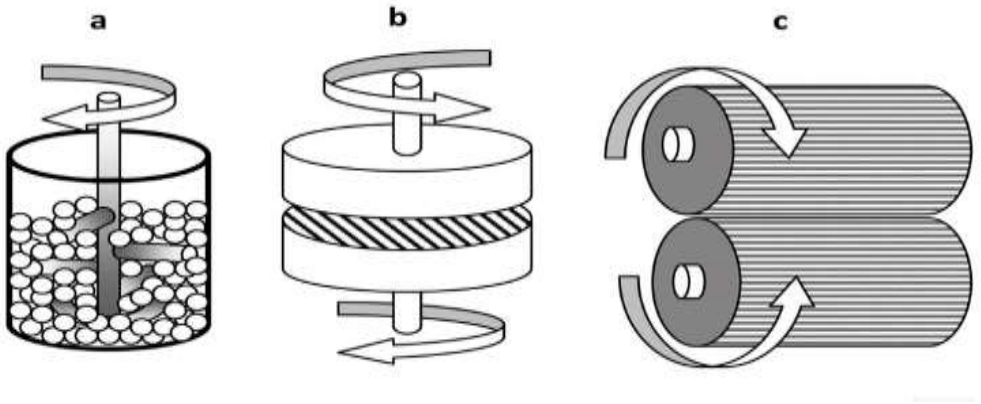

Figure 1 Overview of the mechanical milling machine (Giuliana Gorrasi, 2015)

Bottom up approach:

The bottom-up method is the exact opposite of the top-down method. In this method, the final product is produced by combining raw materials. Namely, by combining molecules and atoms whose dimensions are smaller than Nano, a nanometer is created. In the following, I briefly explain some methods of this approach, which are often used in the synthesis of magnetic nanoparticles. (AZO NANO, 2004)

Sol-gel method:

The sol-gel process is a wet chemical process for the production of mainly ceramic materials from solutions or colloids. In this process, precursors are dissolved in water or alcohol and transformed into a gel by heating and stirring through hydrolysis. (Ehsan Kianfar, 2021) In the next step, the gel is dried, and after the gel is dried, the resulting powder is heated for calcination. A sol-gel process generally involves the following steps:

1 - Mixing of ingredients 2 - Gel formation 3 - Aging 4 - Drying 5 - Chemical stabilization.

Effective parameters in this process include the rate of hydrolysis and condensation reactions, which strongly influence the properties of the final product. Also, parameters such as temperature, type of raw materials and pH are other effective parameters in this reaction. Advantages of the sol-gel method include high purity, low temperature synthesis, accurate control of particle size and good homogeneity. The disadvantages of this method include time-consuming reaction steps, high raw material costs, e.g., for metal alkoxides,

and breaking or wrinkling of the layers due to sudden evaporation. Figure 2 shows an overview of the sol-gel process.

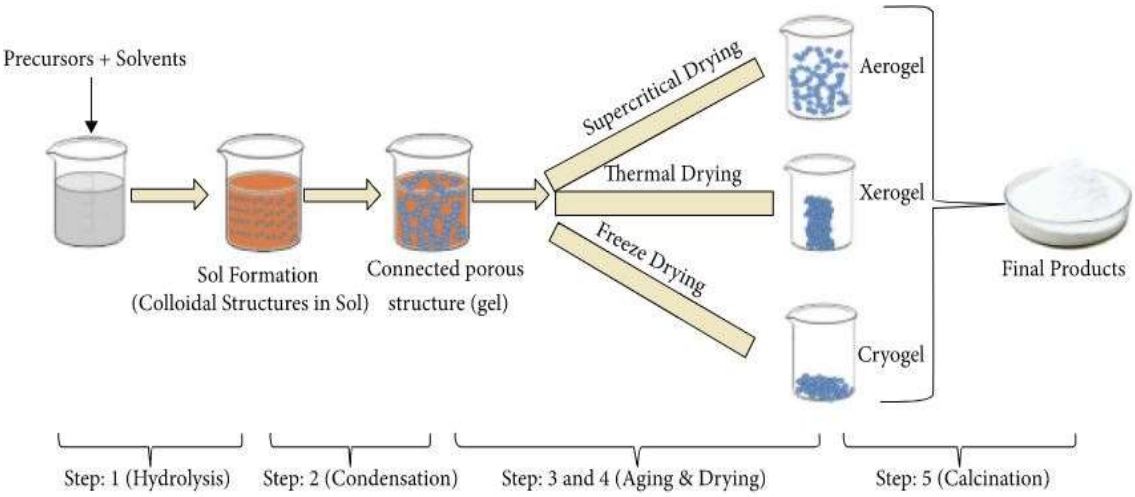

Figure 2 Overview of sol-gel Method (Dmitry Bokov, 2021)

The sol-gel procedure is not a new method, of course. For the first time, in 1800, Ebleman accidentally observed that silicon tetrachloride left in a container first hydrolyzed and then turned into a gel. However, in 1950, extensive studies began in the field of synthesis of ceramics and glass structures using this method.

Thermal decomposition:

One of the methods for the synthesis of nanoparticles is the use of heat to destroy the precursors. There are usually two types of thermal decomposition (WOLFRAM, 2022):

1-With organic surface activators and at low temperature

2-Without using organic surface activators and at high temperature.

Since the second method does not use organic surface activators, a high temperature is required to carry out the reaction. In other words, organic surface activators not only lower the reaction temperature, but also ensure that the particles are well separated and do not agglomerate. (Karin H.Müller, 2014). Effective parameters in this process include temperature, time, type and amount of surface activators, and by controlling these parameters, a pure product can be obtained. The nanoparticles synthesized by this method have advantages such as high crystallinity and narrow size distribution. The size and shape of the nanoparticles are also controlled, but in this method, the nanoparticles must be covered to prevent them from combining with each other.

Despite the superiority of the method of thermal decomposition in the synthesis of ferrite nanoparticles compared to other methods, most of the nanoparticles produced by this method are dissolved only in organic solvents. (JinAh Hwang, 2020). Therefore, after the initial synthesis, complex processes are required to dissolve the nanoparticles in water and make them biocompatible. Moreover, nanoparticles synthesized in this way are not suitable for biological applications due to the use of nonpolar solvents and non-biocompatible activators.

Lee and colleagues, investigated the possibility of using ferrite nanoparticles containing various metals (such as $NiFe_2O_4$, $MnFe_2O_4$ and $CoFe_2O_4$, $ZnFe_2O_4$) synthesized by thermal decomposition and from divalent metal chloride precursors (MCl_2) and in the presence of oleic acid and oleamide surface activators and then tested with DMSA molecules as MRI contrast agents. The results showed that among the ferrite nanoparticles investigated in this study, the $MnZnFe_2O_4$ nanoparticles had the strongest MRI contrast effect (the darkest image) and that the saturation of the magnetism-MRI contrast gradually decreased as M^{2+} changed from Mn to Fe^{2+}, Co^{2+}, and Ni^{2+}.

In another study by Lourdes and his colleagues, ferrite nanoparticles (M: Co^{2+}, Fe^{2+}, Mn^{2+}) were synthesized by thermal decomposition from metal oleate precursors. All modified ferrite nanoparticle colloids were stable in water at pH=7.

Molten salts:

Molten salt production is a suitable method for obtaining nanometer materials with high purity for purposes such as piezoelectric and catalysts. (Santosh K. Gupta, 2021) In this method, reactants and salts are mixed together, and then this mixture is heated to a temperature higher than the temperature of the salts. After cooling, the salts are removed from the product by washing. After removing the salts, the obtained product is dried. This method has advantages such as the production of materials in a short time, the ability to control the shape of the particles and reduce impurities. (YangyangLong, 2014)

Co-precipitation:

The co-precipitation method is one of the oldest methods for the synthesis of nanoparticles. In this method, a solution of chlorides, nitrides, sulfates, etc. is first formed, and then the materials are precipitated with NaOH or Na2Co3 or other bases such as hydroxide, oxalate, or carbonate. Finally, the precipitate is washed, dried, and calcined at a temperature of about 750 °C. (K.Petcharoen, 2012). Iron oxide nanoparticles used for imaging in the last two decades have limitations arising from their fabrication methods. Although the co-precipitation method has advantages, such as cheapness and reaction steps that are not time-consuming, materials synthesized based on this method are generally prepared at a relatively low temperature, resulting in the formation of nanoparticles with low crystallinity and nonuniform particle size distribution.

The non-uniform distribution of particle size can lead to a decrease in the magnetic properties of the material, including its saturation magnetization. Among the research carried out in this field, the study by APA Faiyas. and his colleagues in 2010 should be mentioned. In this study, Fe3O4 nanoparticles were synthesized by the coprecipitation method. In addition, the effects of reaction time and pH on the synthesis of these nanoparticles were investigated. (A.P.A.Faiyas, 2010)

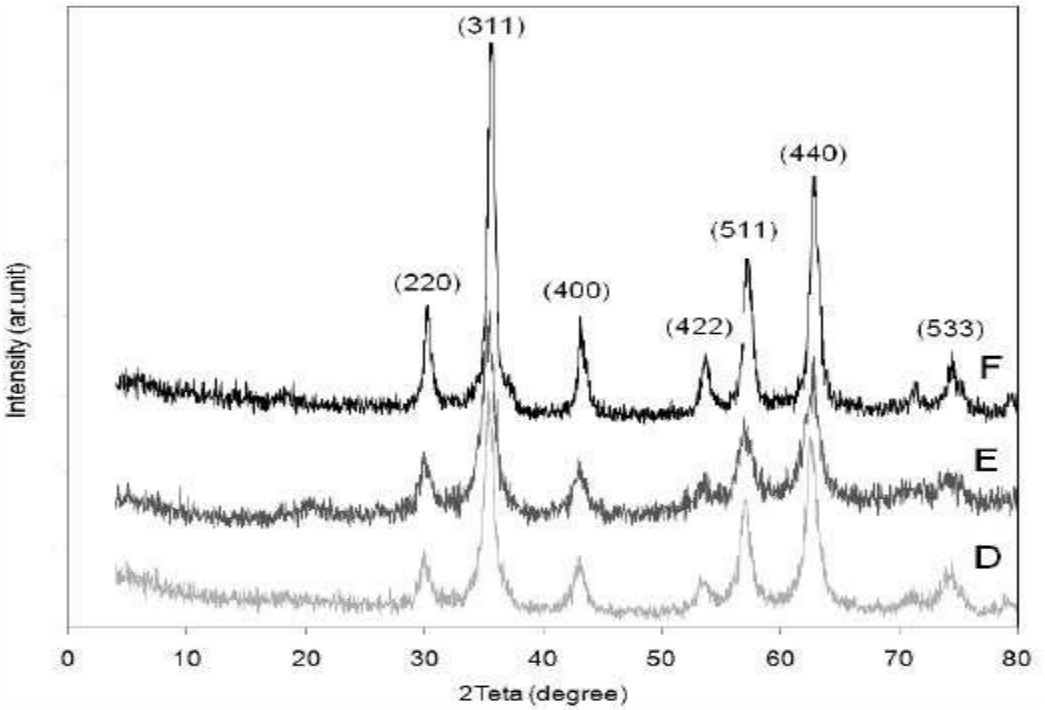

Figure 3: X-ray diffraction pattern of Fe3O4 nanoparticles synthesized by a coprecipitation method (Lakshita Phor, 2019)

Hydrothermal method:

Since this method was used in this study for the synthesis of Mn-Zn ferrite nanoparticles, the description of this method and its history will be discussed. Preparation of nanoparticles by hydrothermal method. One of the fundamental challenges in nanoscience is the precise

control of particle shape and size, which directly depends on the methods of material preparation. As mentioned at the outset, the greatest need is for medical applications such as therapy, biosensors, drug delivery systems, and MRI. They are sensitive to the shape and size of nanomaterials. Therefore, in recent years, solution phase synthesis methods such as hydrothermal synthesis have been proposed as one of the most advantageous methods for the preparation of nanomaterials, and due to the high quality of the products obtained by this method, they are superior to other methods. (Kumhar, 2021)

History of the hydrothermal process:

The word hydrothermal process has a geological origin. The word was first used by an English geologist named Roderick Murchison to describe the action of water at high temperatures and high pressures that leads to the formation of various rocks and minerals. (Kullaiah Byrappa, 2001) The largest single crystals in nature are hydrothermal in origin. At the end of the 20th century, an international conference on hydrothermal processes was held. This conference led to an expansion of information about the thermodynamics of the hydrothermal process.

In the past, the synthesis of magnetic nanoparticles was carried out by hydrothermal methods. For example, the possibility of using these nanoparticles as MRI contrast agents was investigated by Haw and his colleagues. They used $FeCl_3$ and $FeCl_2.4H_2O$ precursors and NaOH to initiate precipitation of Fe_3O_4. Subsequently, Fe_3O_4 nanoparticles were synthesized by a hydrothermal melting process and the prepared nanoparticles were coated with chitosan to improve their stability and biocompatibility. The results of their research show an average particle size of 17 nm, good crystallinity, and a single-phase structure of the synthesized Fe_3O_4 nanoparticles. The result of VSM test in the figure 4 confirms the

superparamagnetic property of the coated nanoparticles. Saturation magnetization 4.57 emu/gr.

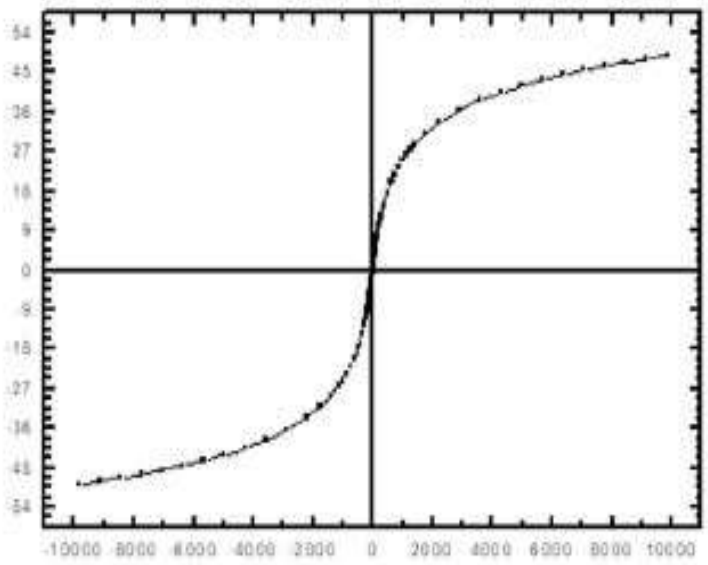

Figure 4: Hysteresis diagram of Fe_3O_4 coated nanoparticles at 289 K (Jinkwon Kim, 2008)

Basics of the hydrothermal method:

The basics of hydrothermal venting are very simple. Hydrothermal reactions are carried out at temperatures above 100 °C and at a pressure above atmospheric pressure in the presence of water. In this process, raw materials such as nitrates, acetates, oxides, hydroxides or metal powders are dissolved in water in an autoclave. After washing and drying, the final product is obtained. (D.O'Hare, 2001)

An autoclave is a device used to generate high temperatures and high pressures to sterilize medical and laboratory equipment and to perform some reactions that require high temperatures and high pressures. (This device was invented by French scientist Charles Chamberland in 1879. A simple autoclave is shown in the figure 5.

Figure 5: General view of a laboratory autoclave (royaniran, 2020)

Advantages of the hydrothermal method:

The advantages of this method include ease, energy saving, low price, better control of nucleation, environmental friendliness (since the reaction takes place in a closed environment), high reaction rate, and low operating temperature. Moreover, the hydrothermal method is suitable to obtain nanoparticles with crystalline nature and consequently high saturation magnetization. (Kumhar, 2021) Since this research work deals with the synthesis of Mn-Zn ferrite nanoparticles for use in medical imaging, it is necessary to briefly introduce the magnetic properties of the material. In the following, different types of magnetic materials, especially soft and hard ferrites, and their hysteresis curves are investigated.

Magnetic properties of materials:

In the 7th century BC, scientists realized that the mineral Fe_3O_4 lodestone, a type of iron ore, can attract small particles of minerals similar to itself and to iron, and this property is now known as magnetism. (Mills, 2010) Iron and some iron alloys are among the best magnetic materials. However, cobalt, nickel and a number of alloys also have magnetic properties. On the other hand, there are materials that are not magnetic and have no magnetic properties. Metals such as gold, silver and copper belong to this category.

Magnetic field vector H:

According to Coulomb's law (the physics classroom, n.d.), the force between two poles m1 and m2 is given by the following relation:

$$F=\frac{km_1m_2}{r_2}r_0$$

where m_1 and m_2 are the intensity of the poles, F is the force, r is the distance between the two poles and r_0 is the vector in the direction of r. Moreover, k is the constant of proportionality whose value is usually equal to one. According to this law, one of the poles generates a magnetic field H instead of the other pole. The unit of the magnetic field is Oersted in CGS and Gauss in SI.

Magnetism:

In general, the dipole moment for any material can be defined and denoted by M. Magnetization is represented as magnetic moment per unit volume. (anurag652, 2021) M is one of the properties of the material and depends on factors such as the magnetic moment of the ions, atoms, or molecules that make it up and the way the dipole moments interact

with each other. In general, magnetization is the sum of magnetic moments per unit volume:

$m = m/ v$

Types of magnetic order and their properties:

Magnetic materials are classified into five categories based on their response to an external magnetic field, including diamagnetic, paramagnetic, ferromagnetic, paramagnetic, and ferrimagnetic. (Moskowitz, 1991) When the particle size becomes smaller than the critical state, other states such as superparamagnetic naturally occur.

Most elements of the periodic table are in two states, diamagnetism and Para magnetism, which are nonmagnetic materials. The state of ferromagnetism does not occur in pure elements, but is observed in compounds such as ferrites. Five categories of magnetic materials are briefly introduced below.

Diamagnetism:

Diamagnetic materials consist of atoms that have no moment because all their orbital layers are filled and there are no unpaired electrons. As long as no external magnetic field is applied to these materials, the magnetization is zero, but by applying an external magnetic field, they produce an induced magnetic field in the opposite direction, which is repelled by the primary field. The fact that the induced magnetic moment is in the opposite direction of the inducing magnetic field is a consequence of Lenz's rule at the atomic level. Organic materials, noble gases, quartz and water are diamagnetic materials. (Moskowitz, 1991) (E. Spain, 2014)

Para magnetism:

In paramagnetic materials, some atoms have a magnetic moment because there are unpaired electrons in their orbitals. In these materials, the magnetic moments are circularly aligned. When an external magnetic field is applied in a particular direction, a series of torques align with the field and produce magnetization; however, when the external field is removed, the magnetization approaches zero. Elements such as magnesium, lithium and molybdenum have paramagnetic properties. (Moskowitz, 1991) (S. Palagummi,, 2016)

Ferromagnetism:

Ferromagnetic materials are materials that can be spontaneously magnetized, i.e., materials in which a magnetic moment is generated in the absence of an external magnetic field. Although not all magnetic moments in a ferromagnetic material point in the same direction, these materials are composed of small sections in which the magnetic moments of each section point in the same direction, but the dipole orientation of each section differs from that of the adjacent section. (Moskowitz, 1991)

Transition metals such as iron, nickel, manganese, and some rare earth metals such as gadolinium have this property. Ferromagnetic materials were first introduced by Weiss in 1907 as the molecular field of ferromagnetic materials. Weiss showed that magnetic bodies consist of domains in which the magnetic moments of the atoms are parallel. (E. Spain, 2014)

Anti-ferro magnetism:

In antiferromagnetic materials we have two sublattices A and B. The magnetic moments in sublattice a are aligned in the same direction. That is, the two sublattices neutralize each

other and the total magnetization becomes zero. When such a material is placed in an external magnetic field, the torques are enhanced in the same direction as the field and the material exhibits weak magnetic properties. Some oxides of manganese, iron and nickel are examples of antiferromagnetic materials. (Moskowitz, 1991) (IMA: Magnet factory and magnetic applications, 2018)

Free magnet:

Ferromagnets consist of at least two separate sublattices a and b, which have antiparallel moments. However, unlike antiferromagnetic materials, these moments are not equal, so the magnetization of the entire material is not zero. The following figure shows the arrangement of magnetic dipoles in a ferromagnetic material. A group of permanent magnets called ferrites belong to this category. The following figure shows the arrangement of magnetic moments in four categories of magnetic materials. (Moskowitz, 1991). Figure 6 shows the four types of magnetic materials.

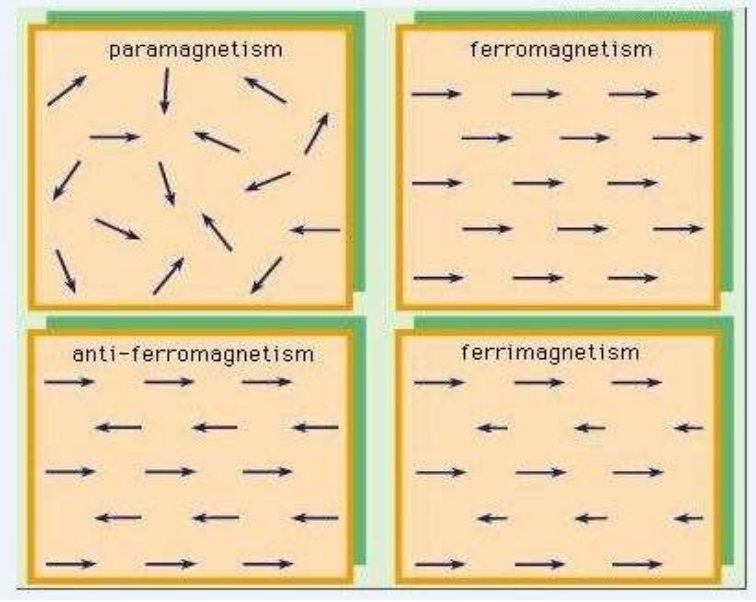

Figure 6: Types of magnetic materials and order of their moments (Awadallah, 2015)

Hysteresis Loop:

In ferromagnetic materials, the generation of external magnetization shifts the domains parallel to the eighth field and these domains become larger. With the further increase of the field, this order has increased so much that it is not completely destroyed even when the field is aligned. The residual magnetization (Mr) is the magnetization that remains after removing a large enough field to reach the saturation magnetization (Ms) where all spins are aligned. As the field is increased, all torques become aligned with the field and the material becomes a single domain. (Abdel-Mohsen Onsy Mohamed, 2018)

At this stage, the magnetization of the material reaches its maximum value, i.e., saturation magnetization. Another characteristic of the hysteresis loop is the coercive field. This refers to the field in which the significance of the field becomes zero. Figure 7 shows the hysteresis loop and the saturation magnetization curve of a ferromagnetic material.

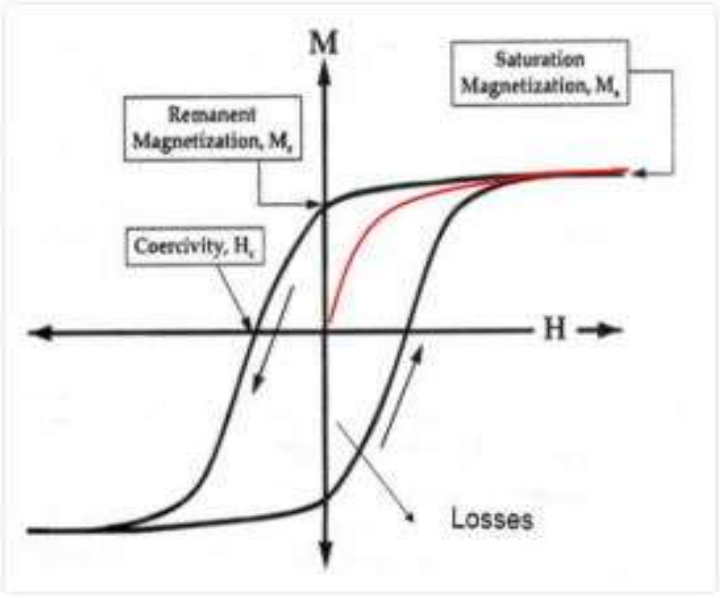

Figure 7: Saturation magnetization curve and hysteresis loop of a ferromagnetic material (MGA, 2012)

The hysteresis curve in ferromagnetic materials can also be interpreted (Magnetic Hysteresis, 2022) using figure 8. One can imagine that every object, before it is brought into an external magnetic field, consists of blocks, each of which has a magnetic field in a certain direction. The total result of these small fields in the object is zero. The blocks whose field direction coincides with the external field H are aligned with it by adding an external magnetic field.

The enlargement of the field causes all the small fields to align with it. In this case, the object reaches its state of saturated magnetization. Decreasing the H-field and bringing it to zero, not all small fields return to their original state, and some of them remain in the same direction as the previous H-field, which corresponds to the state of residual magnetization in the material. (R.C.O'Handleya, 2003). In order for all blocks to return to their original random state, a field opposite to the direction of the original field must be applied to them. Figure 8 shows the effect of field blocks in creating magnetic hysteresis.

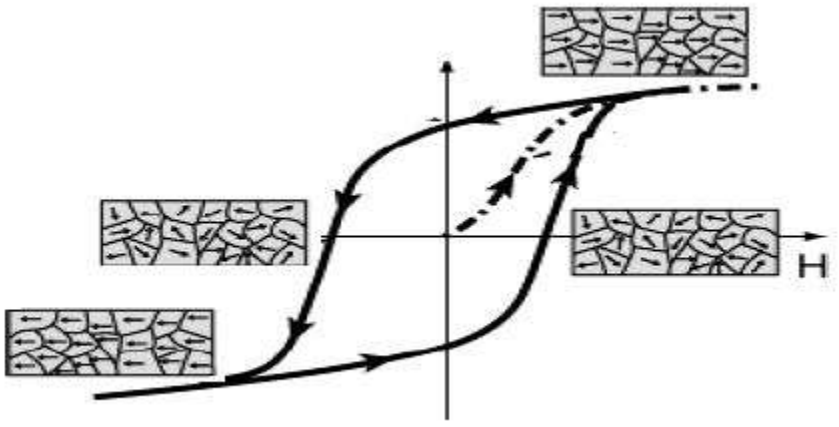

Figure 8: The effect of field blocks in creating magnetic hysteresis (bestknowledgesite, 2016)

Ferrites:

Ferrites are a group of magnetic materials whose main component is iron oxide and which have ferromagnetic properties. It is a ceramic substance consisting of iron oxide (Fe_2O_4) in large quantities combined with metallic elements such as barium (Ba), manganese (Mn), nickel (Ni) and zinc (Zn) in small quantities. Both the iron oxide and the metal are electrically non-conductive and ferrimagnetic. A ferrimagnetic substance is one that has unequal, opposite magnetic moments that allow these materials to maintain spontaneous magnetization. (Sugimoto, 1999) (Daliya S.Mathew, 2007)

These materials are divided into two general categories: 1) soft magnetic ferrites and 2) hard magnetic ferrites. One of the properties of magnetic ferrites is that when they are placed in an external magnetic field, they align with it and do not return to their initial state when the field is turned off. Therefore, they form a hysteresis or hysteresis loop. (Sugimoto, 1999) (Daliya S.Mathew, 2007)

The general formula of ferrites can be written as M(FeO), where M is a divalent metal such as nickel, manganese, copper, barium, yttrium, and so on. As for the material structure, ferrites are polycrystalline materials. This means that they are composed of a large number of tiny crystals with different orientations. In terms of crystal structure, there are different types of ferrites such as spinel, garnet, perovskite, and hexagonal (hexagonal) ferrites. Three main families of ferrites are used to make magnets: hexagonal ferrites, spinel ferrites and garnet ferrites. (Daliya S.Mathew, 2007)

Hexagonal ferrites:

Their general formula is $M(Fe_{12}O_{19})$. Where M is usually barium, strontium or lead. These ferrites are considered magnetically hard magnetic materials. That is, the strength or direction of their magnetic field does not change easily, and they are therefore suitable for making permanent magnets. $BaFe_{12}O_{19}$ (C.Pullar, 2012) (Zuzanna Bielan, 2021)

Spinel Ferries:

Its general formula is $M(Fe_2O_4)$. Here M is one of the metals manganese, nickel, cobalt, zinc, copper or magnesium. They are considered soft magnetic materials. That is, the strength or direction of their magnetic field changes slightly. Therefore, they are suitable for the production of temporary magnets. $NiFe_2O_4$ and $MgFe_2O_4$ (Daliya S.Mathew, 2007) (Zuzanna Bielan, 2021)

Garnet ferries:

Their general formula is M_3 (Fe_5O_{12}). Where M is the metal yttrium (Y) or a rare earth element (lanthanum, cerium, praseodymium, neodymium, promethium, samarium, europium, gadolinium, cyanide, dysprosium, holmium, erbium, toluene, yttrium, glutamine and other scandium). They are considered as hard magnetic materials. $Y_3Fe_5O_{12}$ (S.Geller, 2002)

Due to their properties such as high permeability coefficient, high saturation magnetization and high electrical resistivity, magnetic ferrites have many applications in electronics, telecommunications, computer technology, targeted drug delivery, etc. Cobalt ferrite ($CoFe_2O_4$), for example, is a hard-magnetic ferrite used in magnetic recording

environments due to its high coercive field, as the high magnetic coercive field is necessary to enhance information storage.

Nickel ferrite ($NiFe_2O_4$) is a soft ferromagnetic material with low saturation magnetization and low coercive field, suitable for biomedical applications and ferrofluids. Manganese-zinc ferrite ($Mn_aZn_{(1-a)}\ Fe_2O_4$) has also been considered for medical imaging due to its high saturation magnetization, chemical stability and low price.

Soft ferrites:

This category of ceramic materials has a spinel structure with the general formula MFe_2O_4, where M is a divalent cation such as Ni^{2+}, Zn^{2+}, and Mg^{2+}. Soft magnetic ferrites are easily magnetized by applying a small magnetic field and lose their magnetization easily when the field is interrupted. On the other hand, soft ferrites have low coercivity, so their magnetization is easily changed. Therefore, they have a small hysteresis loop. The characteristics of a small hysteresis loop are a low coercive field, a high saturation magnetization and a low hysteresis magnetization. Soft ferrites have numerous applications in the electronics, computer and medical industries. The most important of these are transformer cores, targeted drug delivery, magnetic heads, and medical imaging. (Sugimoto, 1999) (MarthaPardavi-Horvath, 2000)

Hard ferrites:

Hard ferrites are materials that do not magnetize easily in an external magnetic field and require a larger magnetic field to magnetize them. These materials retain their magnetic moment even after the external field is turned off. (Kirchmayr1, 1996). Therefore, they have a large hysteresis loop. The characteristics of a large hysteresis loop include saturation

temperature, remanent magnetization, and a high coercive field. The hysteresis diagram of soft and hard magnetic materials is shown in the following figure. Due to the high coercive field, hard ferrites are often used in generators, loudspeakers and all kinds of electric motors. Figure 9 shows hysteresis diagram of soft and hard magnetic materials. (Sugimoto, 1999)

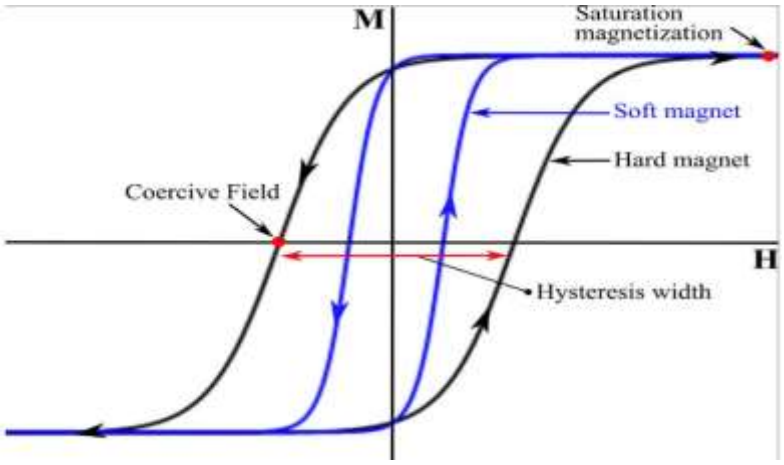

Figure 9: Hysteresis diagram of soft and hard magnetic materials (Ananya Renuka Balakrishna, 2020)

Coating of magnetic nanoparticles:

One of the most important problems associated with the application of nanoparticles in medicine is the lack of stability of nanoparticles in aqueous environments over time. (Stark, 2011).In general, for biological applications, surface coating of nanoparticles is necessary to increase the stability in the biological environment, to better control the particle size, and also for targeted applications such as drug carriers. (Stark, 2011)

Magnetic nanoparticles are stable in acidic or alkaline environments before coating. (Stark, 2011)Therefore, they are not suitable for medical applications. Another disadvantage of

uncoated nanoparticles is the presence of strong dipole-dipole magnetic attractions between the particles in the physiological environment, which causes them to accumulate and therefore be absorbed by plasma proteins and rapidly removed from the bloodstream.

Coating the surface of MNP with organic and inorganic molecules increases the half-life by delaying clearance. (kianfar, 2021)The inner lining network system is active in the liver, spleen and bone marrow and clears them depending on the particle size. Uncoated magnetic nanoparticles are rapidly removed by phagocytic cells. Coating affects the hydrophobicity of the surface charge surface and the pH of these particles, thereby delaying particle clearance. In order to prevent these problems, biocompatible polymer coatings such as chitosan, polyethylene glycol polyvinyl alcohol, dextran, etc. are used, and we will briefly describe each of these polymers below. (Stark, 2011) (kianfar, 2021)

Chitosan:

Chitosan is a natural biocompatible polymer with three molecular weights: low, high and medium. This polymer with molecular formula $C_6H_{11}NO_4$ is obtained from marine sources. (J. Hemapriya, 2019). Chitosan was first discovered in 1895 by Rouget through the reaction of chitin with potassium hydroxide. The figure 10 shows an overview of chitosan-coated ferrite nanoparticles.

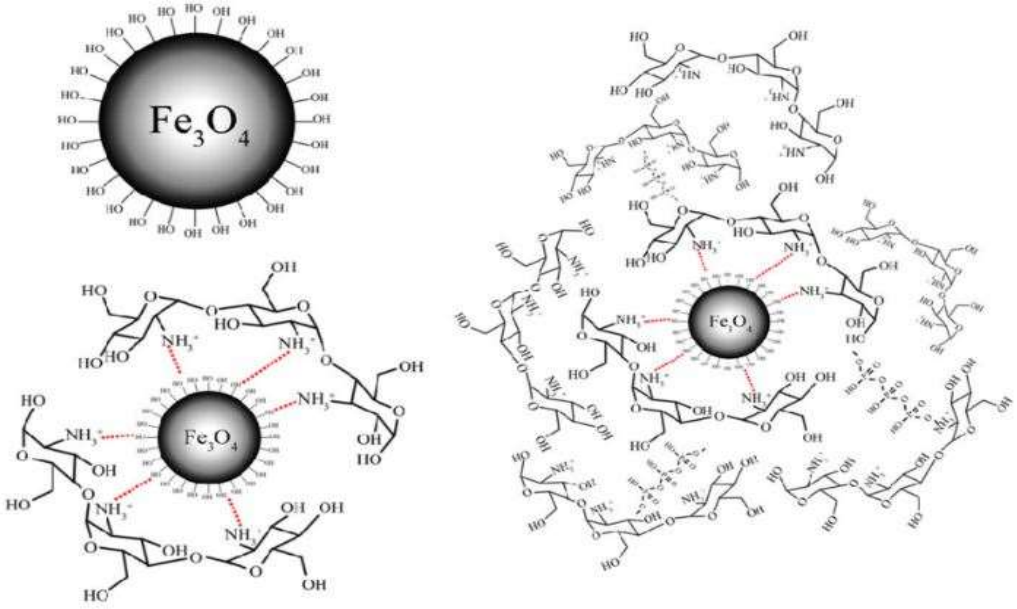

Figure 10: Schema of in situ synthesized chitosan-coated magnetic nanoparticles (CS MNPs) (Rouhollah Khodadust, 2012)

Chitosan is not soluble in water and organic solvents, but can be dissolved in dilute acid solvents such as acetic acid, formic acid, and hydraulic acid. In general, the solubility of chitosan depends on the concentration and type of acid used. Due to its characteristics such as high biocompatibility, acceptable biodegradability, low toxicity and antibacterial properties, it finds good application in drug delivery, wound and burn healing, cosmetics, etc. (J. Hemapriya, 2019)

Chitosan also has the ability to coagulate blood. Studies on chitosan show that even a small amount of this polymer promotes the accumulation of red blood cells. The ability of this polymer to coagulate blood depends on its polymer structure and molecular weight.

Polyethylene glycol (PEG):

Polyethylene glycol is a linear hydrophilic polyether with the molecular formula $H(OCH_2CH_2)$ n OH, where n is the average number of ethylene oxide groups. Polyethylene

glycol is a polymer with a dual property of hydrophilicity and hydrophobicity, which results in nanoparticles coated with this polymer being as soluble in organic solvents such as ethanol, acetone, and chloroform as they are in water. (Christo B. Tsvetanov, 2012)

The average molecular weight of the various forms of polyethylene glycol serves as a distinguishing feature. For example, PEG400 comprises the distribution of polymers with an average molecular weight of 400, where the average number of repeating ethylene oxide groups is 9.9. (Kohnert, R. L, 1993)

Based on the average molecular weight, polyethylene glycols can be liquid or solid under standard conditions. Polyethylene glycols with molecular weights of 200, 300, 400, 600 and 1000 are in liquid form. Nanoparticles coated with this polymer are suitable for medical applications such as targeted drug delivery and magnetic resonance imaging because PEG is a polymer that is biocompatible in the body.

Mn–Zn ferrite nanomaterials:

In the last decade, Mn-Zn ferrites have attracted much attention in academic research because of their beneficial properties. The variation of cation concentration and sintering state changes the electrical and magnetic properties as well as the constructive properties of Nano-ferrites, leading to a wide range of applications. In addition, the morphology, magnetic and electrical properties are affected by the cation distribution in Mn-Zn ferrite. (Preeti Thakur, (2020)) (B. Skołyszewska, 2003)

Among magnetic nanoparticles, Nano-sized Mn-Zn ferrite materials not only have unprecedented size-dependent physical and chemical properties compared to their bulk counterparts, but have also emerged as potential candidates for use in hyperthermia due to

their suitable TC (340 K) and high time- and temperature-dependent permeability stability. Many methods are used to prepare Mn-Zn ferrite nanoparticles, the most common being hydrothermal, precipitation, co-precipitation, combustion, and sol-gel synthesis. (Han-Wen Cheng, 2016) (B. Skołyszewska, 2003)

Compared to larger magnetic particles, magnetic NPs exhibit high magnetic susceptibility. Among the various magnetic NPs (e.g., Fe_3O_4, Fe_2O_3, etc.), Mn-Zn ferrite ($MnZnFe_2O_4$, MZF) has attracted great interest since we reported the synthesis of highly monodisperse and shaped MZF NPs in organic solvents. Interest in the synthesis of MZF-type magnetic NPs to study their functional properties has increased. (H.-J. Qiu a, 2015) (B. Skołyszewska, 2003)

Morphology of Mn-Zn ferrites:

Spinel structure is present in Mn-Zn ferrites. The spinel structure has a main unit cell consisting of 8 subunit cells and has a face-centered cubic (FCC) structure with two types of sites in each unit cell, i.e., tetrahedral (A) and octahedral (B) in the complete structure of Mn-Zn ferrite. 32 octahedral interstitial sites and 64 tetrahedral interstitial sites are present. The spinel structure has an enclosed arrangement of oxygen atoms in which 32 oxygen atoms form a unit cell. The tetrahedral (A) sites are closed by four nearest neighbor oxygen atoms and the octahedral (B) sites have six nearest neighbor oxygen atoms. (Preeti Thakur, (2020)) (B. Skołyszewska, 2003)

In the Mn-Zn spinel ferrite lattice, the Zn ions are located on the tetrahedral sites, while the Fe and Mn ions occupy both tetrahedral and octahedral sites. Due to the spinel structure, different metal ions may be represented, resulting in different magnetic and electrical properties of ferrites. The represented metal ions can enter the spinel crystal lattice by

complementing Fe^{3+} ions and causing the association of these ions at the grain boundary. These morphological properties provide the characteristics of Mn-Zn ferrite nanoparticles that can be tuned as long as the nanoparticle designer chooses synthesis and characterization methods specifically suited for a particular application. In order to achieve the best results from Mn-Zn ferrites for different applications, one must be aware of the different synthesis and characterization methods. (Preeti Thakur, (2020))

Why do we prefer Mn-Zn ferrites?

Mn-Zn ferrites are preferable to other ferrites because they are cost effective and offer a wide range of applications. These ferrites feature voltage insensitivity and low noise and are typically used for applications where a frequency of less than 2 MHz is required. Another advantage of Mn-Zn ferrites is the almost non-existent magneto crystalline anisotropy. (Preeti Thakur, (2020)) (Tao Sun, 2011)

Among all soft ferrites, Mn-Zn ferrites are preferred because of their high permeability, saturation induction, low power losses, and high magnetic induction. Mn-Zn ferrites are of great interest due to their wide range of applications, e.g., hyperthermia applications, power applications, magnetic fluids, high-frequency power supply, storage devices, biomedicine, magnetic resonance, catalysis, etc. The control of the size and shape of Mn-Zn ferrites and the magnetic and morphological properties of Mn-Zn ferrites are continuously improved by the application of various synthesis techniques such as co-precipitation method, sol-gel method, hydrothermal method, conventional ceramic technique, solid-state reaction method, self-combustion method and microemulsion method. The effects of doping on the magnetic and structural properties of the pure Mn-Zn ferrites are also considered. (Preeti Thakur, (2020)) (S.F. Mansour, 2017)

Hierarchical structure:

The hierarchical non-porous metal/metal oxide structure is expected to have a wide range of applications, as nanostructured metal oxides are important functional materials. (Bin Cai, 2015)

The fabrication of hierarchical and self-assembling micro/nanostructures has become an important topic in materials research in recent years. Self-assembly and/or self-aggregation are fundamental mechanisms by which different motifs for nanoparticle arrangement or even densely packed periodic structures are formed in materials by the spatial arrangement of their basic building blocks. The assembly is governed by forces determined by competing non-covalent intraparticle or intramolecular interactions. The hierarchical structures formed by the assembly of nanocrystalline building blocks offer new opportunities to optimize, tune, and/or improve the properties and performance of the materials by increasing the specific surface areas. (Yao-Ming Hao,, 2012) (Sapna, 2018)

Applications of ferrite nanoparticles:

Due to their special magnetic properties, magnetic iron oxide nanoparticles are of great interest in various fields, such as magnetic recording, magnetic resonance imaging, targeted drug delivery, electronic devices, and environmental cleaning. Below are some examples of these applications. (IbrahimKhan, 2019)

Targeted drug delivery:

Targeted drug delivery is a series of actions that cause drug accumulation in a specific part of the body. (SemaÇalış, 2019) The original idea of using magnetic nanoparticles for

targeted drug delivery originated in the late 1970s. In this method, the entire drug or magnetic carrier enters the body through venous or arterial vessels, and with the help of an external magnetic field and the creation of a magnetic gradient in a specific part of the body (Manjeet S.Dahiya, 2018), the entire drug or magnetic carrier is transported to that location through the bloodstream. (SemaÇalış, 2019) Theoretically, any drug delivery system should have two main features. 1) Increase the efficacy of the drug in the target tissue 2) Decrease the toxicity of the drug in other tissues of the body.

Targeted drug delivery can also be used to treat cancer. When the transfer and accumulation of particles occurs at the tumor, the drugs are separated from their magnetic carriers and released. (Manjeet S.Dahiya, 2018) Due to the difference in pH between healthy tissue (neutral pH) and cancerous tissue with acidic pH, the drug or magnetic carrier is selected to be sensitive to the acidic pH and released at the tumor site. The disadvantage of this method is that it is time consuming.

Magnetic ferrite nanoparticles in MRI:

In recent decades, due to the development of nanotechnology, magnetic nanoparticles, including iron oxide (ferrites), have been considered as a strong contrast agent in MRI imaging. (Ashish Avasthi, 2020).Nanoparticles are widely used in medicine, especially in cancer diagnosis and magnetic resonance imaging. (Guadalupe Gabriel Flores-Rojas, 2022) This application is due to the strong accumulation of these particles in tumor tissues (due to their biocompatibility and increased permeability and survivability in tissues). In addition, nanomaterials remain in the blood longer than other materials, which can lead to the accumulation of the medical agent bound to them in the target tissue.

Ferrite nanoparticles are used in part because they are nontoxic, do not induce an immune response, are small, have high magnetic properties, and can adapt to the organs of a particular target by changing the thickness of the shell. (Seipati Rosemary Mokhosi , 2022).In endogenous applications, iron oxide nanoparticles with a core of Fe_3O_4 (or α-Fe_2O_3) with an organic or inorganic coating) are used as negative contrast agents in MRI imaging.

These compounds can also cause the image of the target tissue to become darker, which is also due to the mixing of the relaxation time of water. Nowadays, magnetic nanoparticles, especially spinel ferrite nanoparticles with the general formula MFe_2O_4, are used in most medical applications. (Guadalupe Gabriel Flores-Rojas, 2022) For example, metal ferrite nanoparticles substituted with manganese and zinc with the general formula $Mn_aZn_{(1-a)}$ Fe_2O_4 show the strongest contrast effect.

History of MRI:

In 1946, Edward Purcell and Felix Bloch independently discovered nuclear magnetic resonance (NMR), the basis for magnetic resonance imaging (MRI). In 1952, Edward Purcell and Felix Bloch were jointly awarded the Nobel Prize in Physics for their discovery. (Rinck, 2008)

The next important milestone was reached in 1969 when Dr. Raymond Damadian theorized that cancer cells could be detected using nuclear magnetic resonance. (Raymond Damadian, 1974)Raymond Damadian published the results of his experiments in 1971, which proved the accuracy of his theory. Also, in 1971, Paul Lauterbur developed a method to obtain two- and three-dimensional images of living tissue using NMR. (Rinck, 2008) (national MAGLAB, 2012-2022)

The following year, Lauterbur used his NMR technique to examine two test tubes (one with normal water, the other with heavy water) and was able to produce an accurate cross-sectional image of the test tubes. His work was accepted and published by Nature in 1973. In 1973, Peter Mansfield published his research paper on the use of magnetic field gradients to produce three-dimensional images of MRI. (Mansfield, 2003)

In 1977, Dr. Raymond Damadian built the first whole body scanner for humans called "Indomitable" and performed the first whole body MRI on a patient. Raymond Damadian's company (FONAR) introduced the world's first commercial MRI scanner in 1980. (national MAGLAB, 2012-2022) In 2003, Paul Lauterbur and Peter Mansfield were jointly awarded the Nobel Prize in Physiology and Medicine for their contributions to the development of magnetic resonance imaging. (Mayor, 2003)

The basics of MRI:

An atomic nucleus with an odd number of neutrons and protons forms a magnetic pole. Living tissue consists mainly of water molecules. (Schenck, 2003) This is because 70% of the body is filled with water. Each water molecule consists of two hydrogen nuclei with strong magnetic poles. Normally, these magnetic poles are aligned diagonally and cancel each other out. (Mansfield, 2003)

The function is based on the magnetic resonance of the nucleus and the slowing down of the spins of the protons exposed to a strong magnetic field. By applying a very strong external magnetic field, the spins of the nuclear protons are all aligned either parallel or antiparallel to the external field. During the alignment, the spins are exposed to the Larmor frequency ($\omega 0$). When certain radio waves are irradiated into the body, a radio frequency (RF) enters the body and is absorbed by the hydrogen protons, causing the protons to

absorb energy and change their polarization. When the radio waves are removed, the out-of-equilibrium protons return to their original state and a photon is released. This photon is detected and converted into an image. (SPIN PHYSICS, 2020)

In MRI imaging, there are two options:

1-Spin-lattice relaxation time 2. spin-spin relaxation time.

In other words, T_1 is the time when 63% of the network returns to its equilibrium state, and T_2 is the time when 37% of the protons are not yet in the equilibrium state. (SPIN PHYSICS, 2020)

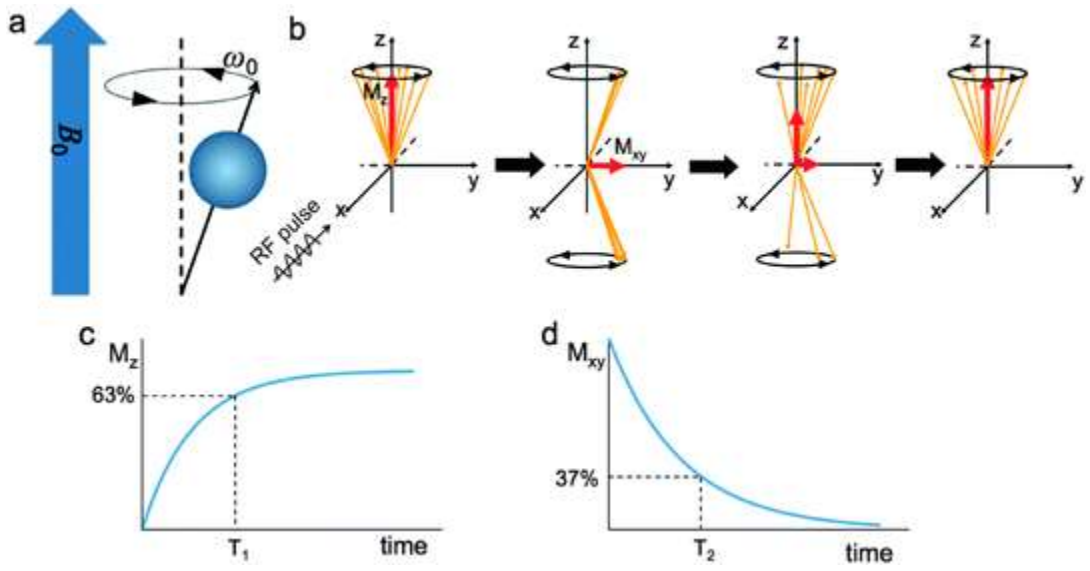

Figure 11: Principles of magnetic resonance imaging (MRI). (a) In magnetic field, the hydrogen nuclear spins align with (parallel) or against (antiparallel) the external magnetic field. (b) Irradiation of resonant RF results in decrease in longitudinal magnetization (M z) and generation of transverse magnetization (M xy). Subsequently, the nuclear spins return to their initial state, referred to as relaxation. (c and d) T_1 is the time required for longitudinal magnetization to recover to 63% of its equilibrium (c), and T_2 is the time required for transverse magnetization to drop to 37% of its initial magnitude (d). (Gayathri Thirumalraj, 2015)

MRI Applications:

MRI, or magnetic resonance imaging, is one of the most advanced medical imaging methods. With this method, one can see the image of the internal tissues of the body, and thus problems and diseases of the body organs can be diagnosed. (Magnetic Resonance Imaging (MRI), 2022)

In X-ray imaging methods such as plain X-ray or CT-scan, the body is exposed to a certain amount of ionizing radiation, which can cause problems in cell function if it exceeds a certain limit. MRI does not use X-rays; therefore, it is much less harmful than X-rays and CT. (Magnetic Resonance Imaging (MRI), 2022)

Although MRI images have high resolution, they do not have the contrast necessary to distinguish between healthy tissue and tumors. Therefore, the use of contrast agents in this imaging modality improves the quality and thus the diagnosis of healthy tissue and tumors. (Clare, 1997)

MRI has the advantage over other imaging modalities in that it provides detailed images of the soft tissues of the body. Another advantage of this method is dynamic imaging, as images can be acquired continuously, which is comparable to dynamic examinations such as heart rate imaging. The following figure shows an overview of whole-body MRI. MRA is now used in the diagnosis of many diseases and lesions of various body organs, including the brain, heart, neck, spine, seals, etc. (Clare, 1997) (Magnetic Resonance Imaging (MRI), 2022). Figure 12 shows the whole-body MRI image.

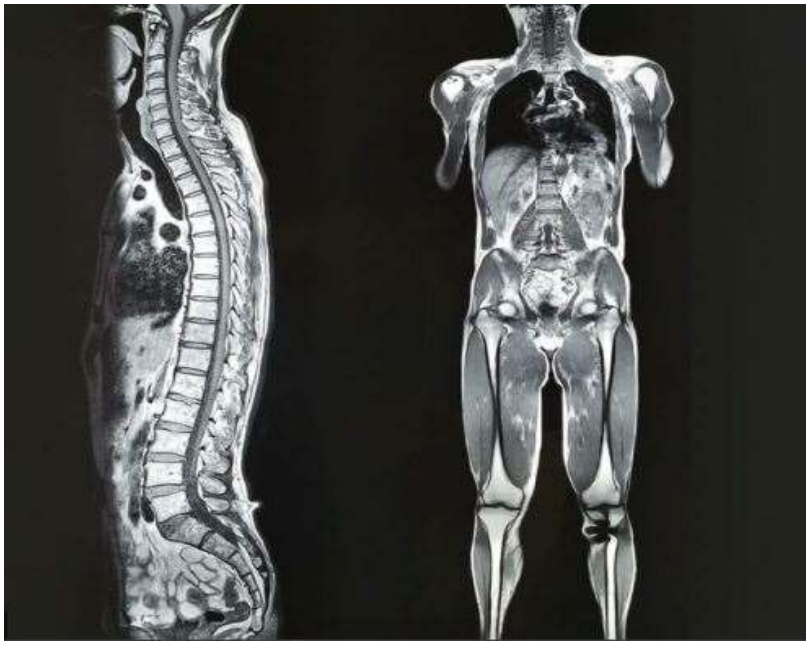

Figure 12: whole body MRI view (MEDICOVER, 2022)

MRI of the brain:

Magnetic resonance imaging (MRI) of the brain uses a strong magnetic field, radio waves, and a computer to produce images of the brain and other parts of the skull that are much clearer and more detailed than images taken by other methods. (Brain MRI, 2022) MRI Imaging of the head is used to investigate sudden onset or chronic symptoms. It is used to diagnose diseases such as the following:

Brain tumors, stroke, brain infections, developmental abnormalities, hydrocephalus, causes of epilepsy and convulsions, causes of headaches, dizziness, weakness and constant diplopia, cerebral hemorrhage in patients with brain trauma, some chronic diseases such as MS, visual and inner ear disorders, pituitary gland disorders, vascular problems such as cerebral aneurysm, blockage of blood vessels or venous thrombosis (formation of a blood clot in a vein). (Brain MRI, 2022)

MRI of the spine:

This method is usually used to study abnormal disc swelling, spinal stenosis, etc. In addition, this type of imaging is the best method to check the status of recurrent injuries in patients who have recently undergone surgery. (Radiological Society of North America, 2022)

Imaging of fine structures:

Researchers have succeeded in increasing the resolution of MRI imaging by a factor of 100 million. They believe this method is so powerful that bacteria, viruses and proteins can be observed. This development is based on the MRFM (magnetic resonance force microscopy) technique, which can detect very small magnetic forces. In addition to the high resolution of the image, MRAF has the advantage of being able to see beneath the surface. It is also possible to obtain 3D images of biological objects in the nanometer range.

The effect of "MRI" in predicting heart attacks:

Johns Hopkins University researchers found that MRI scans of the carotid arteries can predict cardiovascular disease. (British Heart Foundation, 2016). American researchers recently found that MRI scans of the carotid arteries, which supply blood to the brain, provide a more accurate and reliable assessment of the risk of stroke and other cardiovascular disease than ultrasound scans.

MRI can measure macrophages, or white blood cells, in the blood, according to studies published in the 2007 16th issue of the U.S. National Academic Progress Journal. With

these detailed images, researchers can not only study macrophage activity, but also show whether or not macrophage activity is unstable and causing a heart attack.

The aim of the research:

As mentioned above, the aim of this research is to synthesize hierarchical manganese-zinc-ferrite nanoparticles with the following formula ($Mn_{0.5}Zn_{0.5}Fe_2O_4$) by a hydrothermal process and to coat these nanoparticles with biocompatible polymers such as polyethylene glycol. After the initial synthesis of the nanoparticles, the effect of the hydrothermal process parameters such as time and pH will be studied in order to optimally improve them.

Chapter 2

Materials and methods:

In the first chapter, the hydrothermal method was presented as one of the methods of nanoparticle synthesis and the factors affecting it were studied. Also, suitable coatings were presented to increase the stability and bioavailability of nanoparticles. Finally, the basic principles of MRI work were explained in detail. Consumables, suitable laboratory methods for synthesis and coating of Mn-Zn ferrite nanoparticles, and methods for characterization are presented. The associated section also lists all the equipment used in the synthesis along with its equipment and technical data.

Consumption materials:

The list of materials used in this research is given in Table 1.

Consumption materials	chemical formula
Iron Nitrate	$Fe\ (NO_3)_3.9H_2O$
Manganese Nitrate	$Mn\ (NO_3)_2.\ XH_2O$
Zinc Acetate	$Zn\ (CH_3COO)_2.2H_2O$
Pure Urea	$CO(NH_2)_2$
Ammonium Fluoride	NH_4F
Hydrogen Peroxide	H_2O_2, 30%
Ammonia Solution	NH_3, 25%
Nitric Acid	HNO_3, 65%
Ascorbic Acid	$C_6H_8O_6$
Ferric Chloride	$FeCl_3.6H_2O$
Zinc Chloride	$ZnCl_2.$
Manganese Chloride	$MnCl_2.4H_2O$

Table 1: List of Consumption Materials

Synthesis of nanomaterials:

This section presents the synthesis of Mn-Zn ferrite nanoparticles by a hydrothermal process and their subsequent coating with polyethylene glycol (PEG).

First Experiment:

In the typical synthesis of Mn-Zn ferrite nanoparticles, 2.232 gr Fe $(NO_3)_3$. $9H_2O$, 0.366 gr Zn $(CH_3COO)_2.2H_2O$, 0.358 gr Mn $(NO_3)_2$. XH_2O, 4.80 gr CO $(NH_2)_2$, and 0.7 gr NH_4F were subsequently dissolved in 30 mL deionized water (18.2 MΩ-cm resistivity) with stirring at room temperature.

The pH was measured in three different steps: first by adding 3 salts (pH=1.7), then by adding urea (pH=2.3), and finally by adding NH_4F (pH=4.8). In the first test, 0.1 M nitric acid (HNO_3) was added dropwise to the solution after stirring for 10 minutes, until the pH was adjusted to 3. (Bin Cai, 2015).Then I adjusted the pH from pH=4 to pH=10 by adding NH_3 at the rate of 1 unit per day. The homogeneous solution was then transferred to a 50-mL stainless steel autoclave lined with Teflon. The autoclave was sealed and maintained at 180 °C in an electric oven for 20 hours. After natural cooling to room temperature, the precipitate was collected and rinsed several times with deionized water and ethanol. The test was repeated 8 times at pH 3, 4, 5, 6, 7, 8, 9 and 10 to obtain the best result according to XRD analysis. Figure 13 shows the synthesized materials at different pH values.

Figure 13: synthesis with different pH

The XRD results of this synthesis showed that we obtained Fe_2O_3 instead of Fe_3O_4. We know that Fe_2O_3 is a paramagnetic mineral that has only Fe^{2+} oxidation state, while Fe_3O_4 is a ferromagnetic material that has both Fe^{2+} and Fe^{3+} oxidation states. According to the above description, the XRD result of this synthesis was not appropriate. Therefore, it was considered as an experiment leading to failure.

Second Experiment:

Here, ascorbic acid and urea play an important role in the formation of $Mn_{0.5}Zn_{0.5}Fe_2O_4$. First, 3.24 g $FeCl_3$, 0.65 g $ZnCl_2$, and 0.97 g $MnCl_2$ were dissolved in deionized water, and then 3.17 g ascorbic acid and 3.3 g urea were added. The prepared solution was then stirred at room temperature for 30 minutes. This mixture was then transferred to a Teflon-lined stainless-steel autoclave at 160 °C for 6 hours. The resulting precipitates were then dried at 70 °C for 10 hours followed by annealing at 500 °C for 2 hours. The pH was measured

in three different steps: first by adding 3 salts (pH=1.7), then by adding ascorbic acid (pH=1.12), and finally by adding urea (pH=1.30).

Figure 14: after adding 3 salts. pH reached to 1.7

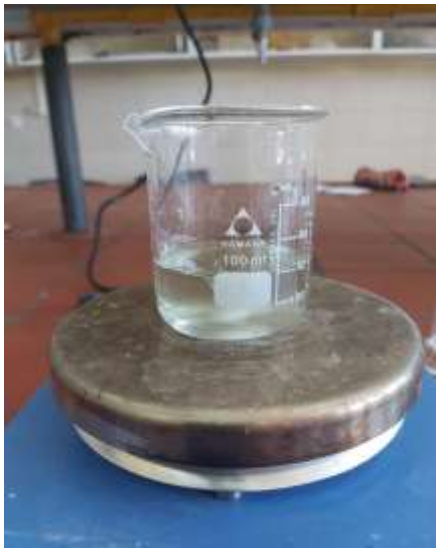

Figure 15: After adding ascorbic acid pH reached to 1.12

Figure 16: after adding urea pH reached to 1.30

Figure 17*: the cooled solution* was collected and rinsed with deionized water and ethanol several times.

Figure 18: The resulting precipitates after annealing for 500˚C for 2 hrs.

I also performed the typical synthesis of Mn-Zn ferrite nanoparticles by dissolving 3.24 g $FeCl_3$, 0.65 g $ZnCl_2$, and 0.97 g $MnCl_2$ in 30 mL deionized water (18.2 MΩ-cm resistivity) with stirring at room temperature. I then adjusted the pH from PH =1.7 to pH=10 by adding NH_3. The homogeneous solution was then transferred to a stainless steel 50-mL autoclave lined with Teflon. The autoclave was sealed and held at 180 °C in an electric oven for 3 hours. After natural cooling to room temperature, the precipitate was collected and rinsed several times with deionized water and ethanol.

Figure 19: after adding 3 salts

Figure 20: controlling pH after adding NH_3

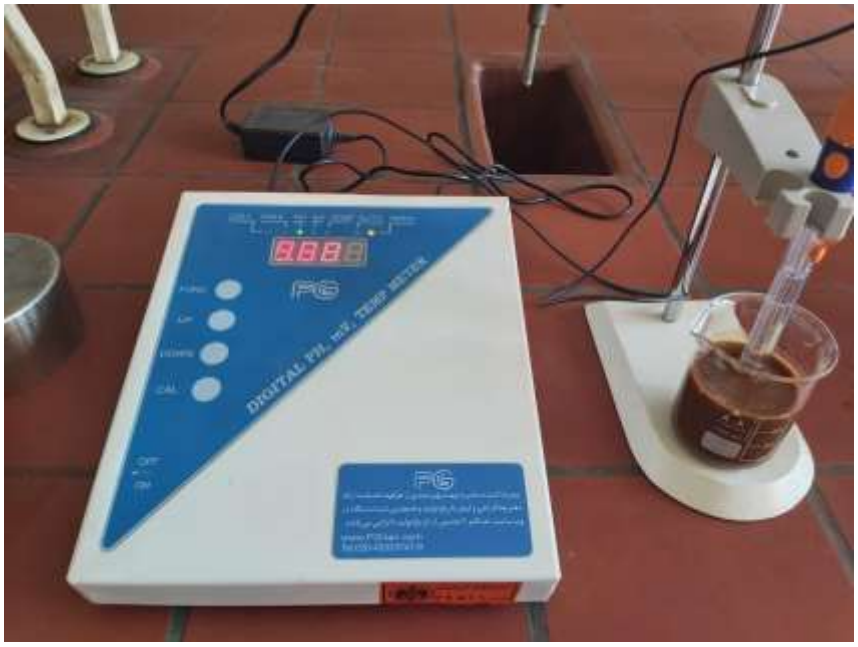

Figure 21: By adding NH_3, I adjusted the pH from PH=1.7 to pH=10

Surface coating of synthesized nanoparticles with pegs by physical bonding method:

To coat manganese-zinc-ferrite nanoparticles with polyethylene glycol by physical bonding method, 0.5 g of both nanoparticles (normal and hierarchical) synthesized by hydrothermal method were first mixed in 50 ml of distilled water at room temperature for 30 min in an ultrasonic bath. Also, 2 g of polyethylene glycol was poured into 50 ml of double distilled water and stirred with a magnetic stirrer for one hour. Then, this solution was added to the previous suspension and stirred on a shaker at 700 rpm for 24 hours. After separation by centrifugation, the coated nanoparticles were dried at room temperature for one day. The following figure shows the mechanism of attachment of PEG to ferrite nanoparticles. In Figure 22 we see how PEG binds to nanoparticles.

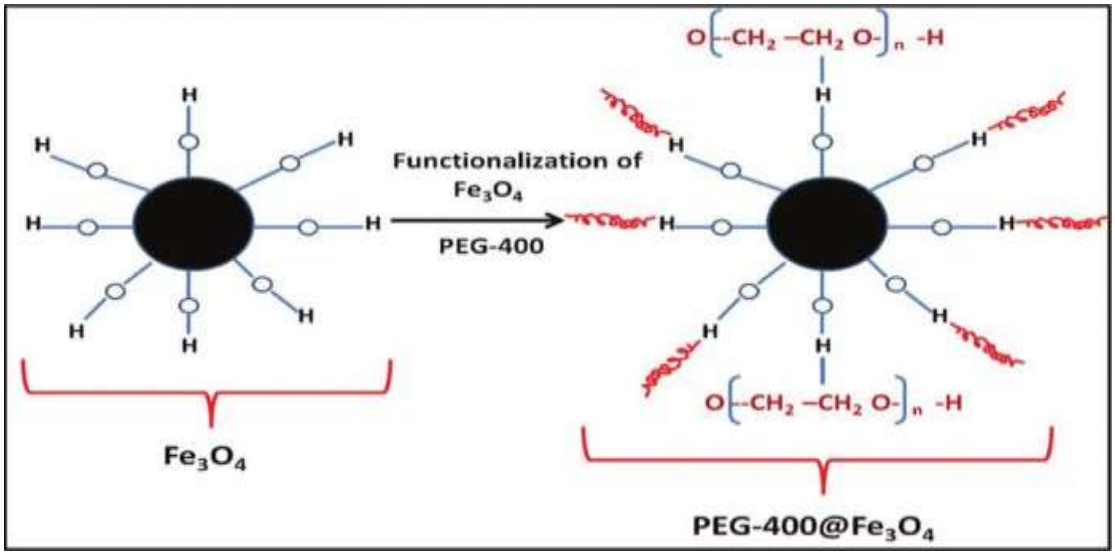

Figure 22: The mechanism of binding PEG polymer to magnetic nanoparticles

Characterization:

In this study, various analyzes were performed to characterize the synthesized zinc hierarchical manganese ferrite nanoparticles coated with polyethylene glycol, which are briefly discussed below.

XRD Analysis:

In order to analyze and determine the properties of the crystals and identify the phases in the samples, XRD analysis of the D8 Advance was performed. As we know, the design principles of the XRD instrument are based on the irradiation of X-rays onto the sample at different angles and the analysis of their diffraction or reflection pattern. Therefore, X-rays with a wavelength of N Angstroms were used in all tests. The time remaining in each second increment and the size of each increment of degree and the scan range between degree and degree were chosen. In addition, XRD analysis by the Rietveld method was used to determine the size of the network parameters and the percentage of phases.

SEM Analysis:

The German-made scanning electron microscope Sigma VP -500 from the company ZEISS was used to image the samples and determine their surface characteristics and morphology (size, shape, and particle size distribution), as well as the chemical composition of the obtained samples.

FTIR Analysis:

This analysis is used to identify the excellent compounds of a substance (identifying their functional groups) and also to compare the compounds in two organic substances with the same base. With this technique, the intensity of the infrared spectrum can be determined based on the absorption wavelength. In this study, the JASCO-6300 instrument manufactured in Japan was used.

TEM Analysis:

One of the most effective methods is to check the morphology (shape and size) of nanoparticles coated with polyethylene glycol, which can provide us with useful quantitative and qualitative information. The TEM test is a method that allows direct imaging of particles down to the size of an atom, and this advantage of direct imaging should be considered when working with a microscope. A German-made transmission electron microscope (TEM) (EM10C) from ZEISS was used for this test.

DLS-ZETTA Analysis:

The Horiba SZ-100 instrument manufactured in Japan was used to determine the size distribution of particles in suspensions. To prepare samples of pure zinc-manganese ferrite nanoparticles and zinc-manganese ferrite nanoparticles coated with polyethylene glycol, 1 milligrams of the synthesized powder were distributed in 1 ml of distilled water. To achieve complete uniformity, the samples were placed on the stirrer for one hour.

ICP-mass Analysis:

To determine the percentage of the elements iron, manganese and zinc in the synthesized nanoparticles, the device PQ 9000 of the company Analytik Jena from Germany was used.

VSM Analysis:

To measure the magnetic properties of the synthesized powders, a magnetometer for vibrating samples manufactured by the Iranian company Meghnatis Daghigh Kavir was used to indicate a maximum field. The magnetic properties were also studied at room temperature.

Blood compatibility:

A blood sample was collected from a healthy human volunteer. The synthesized PEG - coated and uncoated NPs at concentrations of 0.1, 0.2 and 0.3 mg/ml were added to the blood samples and the following tests were performed:

1- Complete blood count (CBC) studies

2- In vitro blood clotting studies (PT & αPTT).

MRI Test:

Magnetization of the samples was performed using ingenious Philips model MRI machine. Imaging of Fe_3O_4, $MnZnFe_2O_4$, Fe_3O_4/PEG and $MnZnFe_2O_4$/PEG nanoparticles in distilled water solution with a concentration of 0.1, 0.2 and 0.3 mg/ml was done. In order to measure the T_2 time, the materials were placed in tubes in the MRI machine with a magnetic field of 1.5 Tesla.

Chapter 3

Results and Discussion:

In this chapter, the results obtained from the experiments and the discussion about them are presented. First, the results of the XRD, SEM, FTIR, TEM, DLS-ZETA, and ICP analyses of the Fe_3O_4 and $Mn_{0.5}Zn_{0.5}Fe_2O_4$ samples are examined. Then, the results of the investigations of PEG -coated Mn-Zn ferrite samples by XRD, FTIR and TEM -tests are presented. Finally, the results of VSM, MRI and biocompatibility tests for all 4 samples are presented for comparison.

The characteristics of the synthesized samples and the results of the XRD examination are shown in Figures 23 and 24. The patterns are consistent with those of the synthesized samples. Examination of the XRD patterns shows that the Mn-Zn ferrite was synthesized correctly.

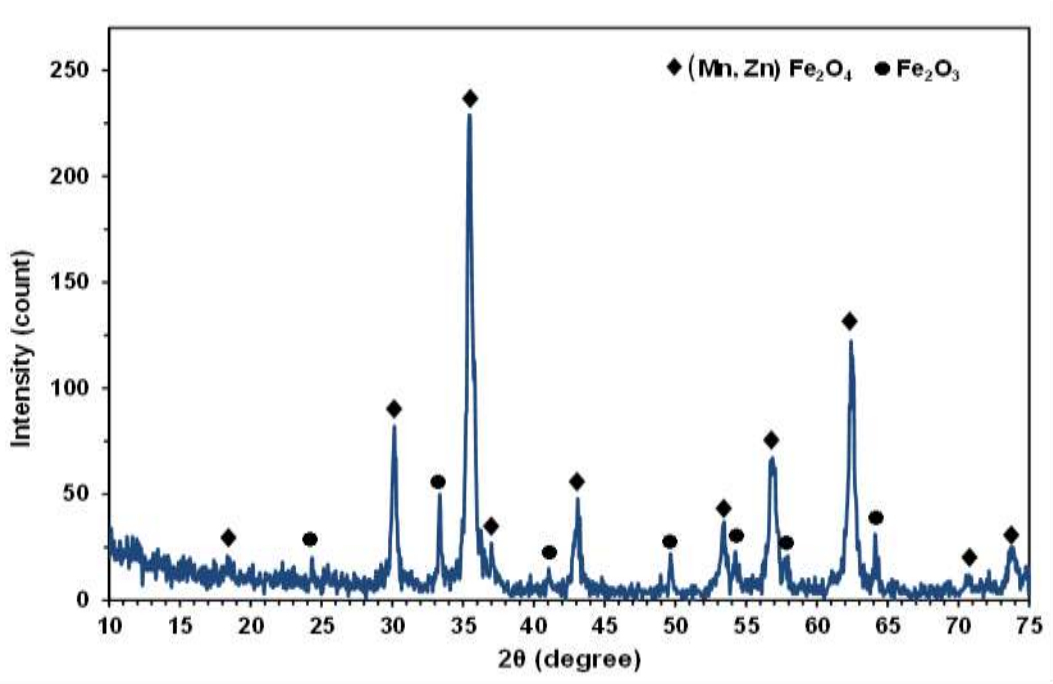

Figure 23: XRD Of Mn-Zn Ferrite NPs

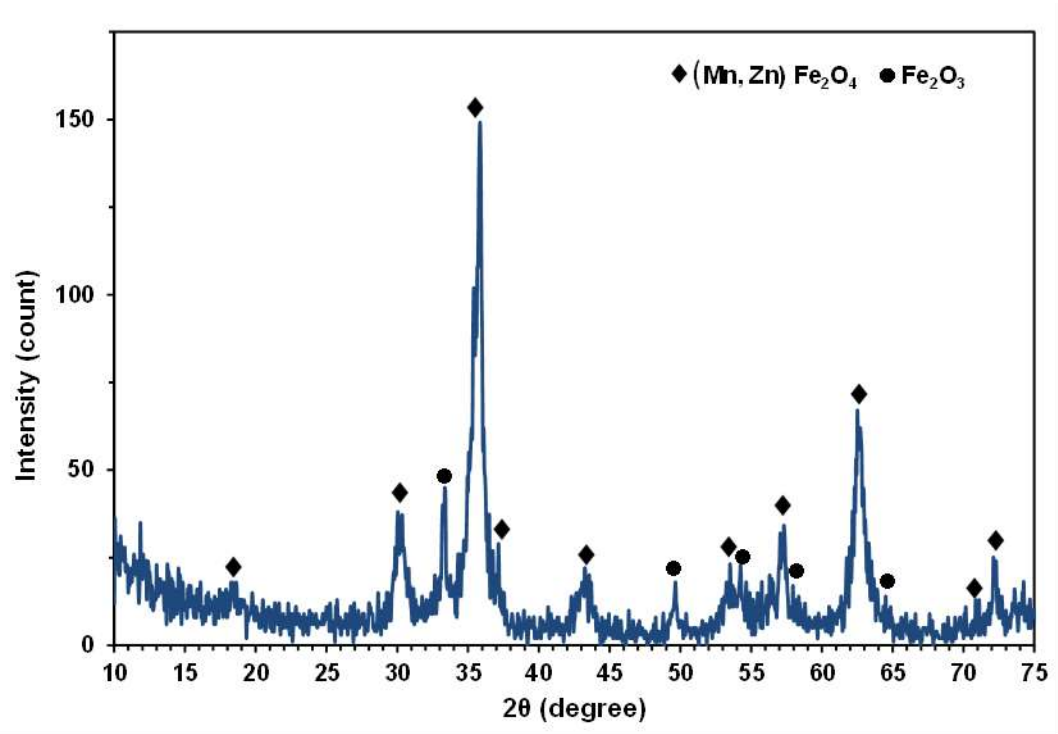

Figure 24: XRD- Hierarchical Mn-Zn Ferrite NPs

SEM Analysis:

Figures 25 and 26 show the SEM image of normal ferrite and hierarchical ferrite. As you can see, the particles are lumpy. Also, the particles are almost spherical and have a relatively uniform distribution. The measurements (by averaging the size of the nanoparticles in the images from SEM show that the average size of the particles is about 50 and for this reason the XRD patterns shown in the figures 23 and 24 are wider than the standard pattern.

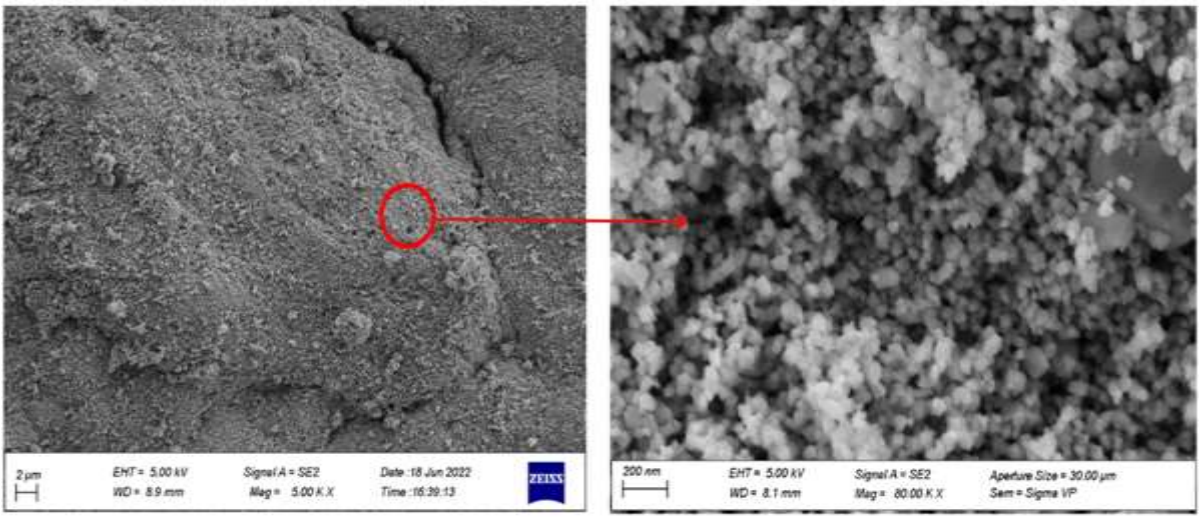

Figure 25 : SEM-Mn-Zn Ferrite NPs

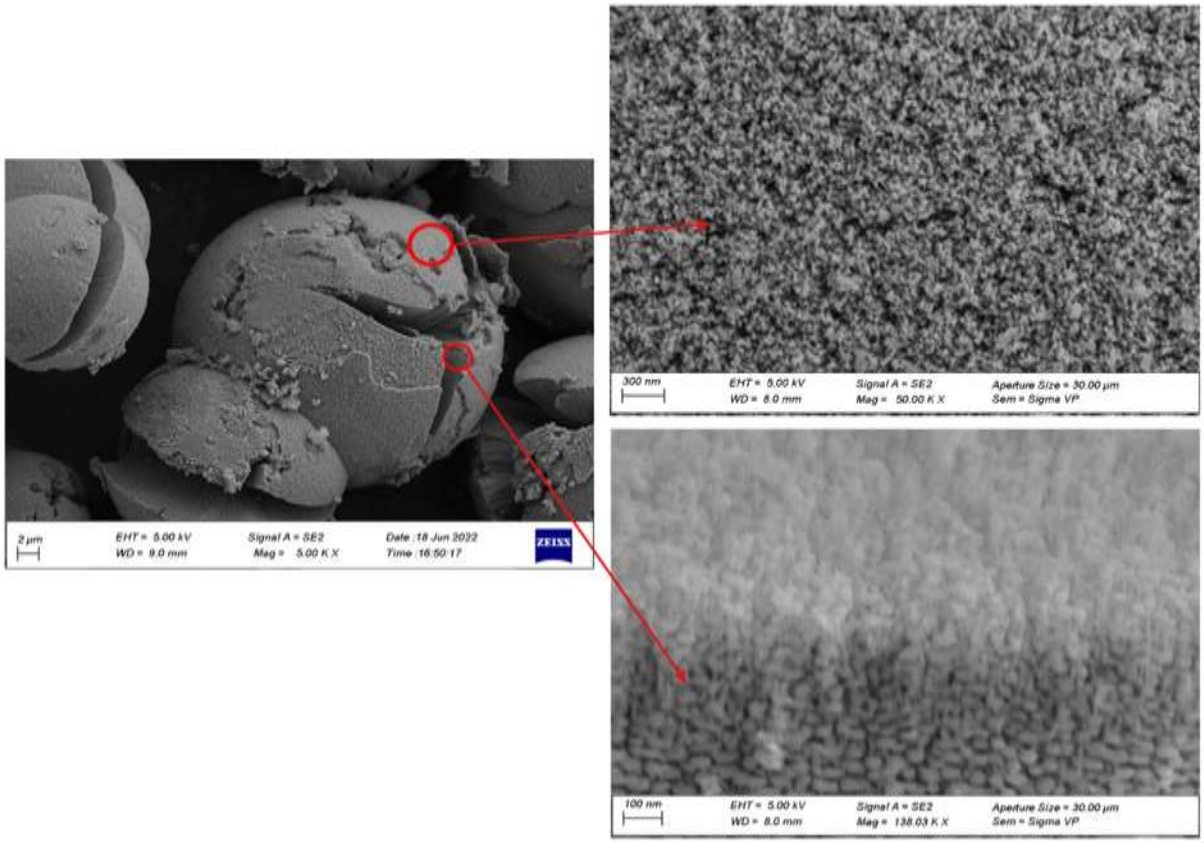

Figure 26: SEM- Hierarchical Mn-Zn Ferrite NPs

TEM Analysis:

To verify the morphology (shape and size) of the coated nanoparticles, an TEM analysis was performed. The results of this analysis are shown in Figures 27 and 28. As can be seen from the figures, the nanoparticles coated with PEG are almost spherical and have the same size distribution. Moreover, almost all particles are 60 nm in size. Some uncoated nanoparticles have only a black crystalline core, but the nanoparticles coated with PEG have a light gray shell around the core in addition to the black crystalline core. The shell represents the PEG shell.

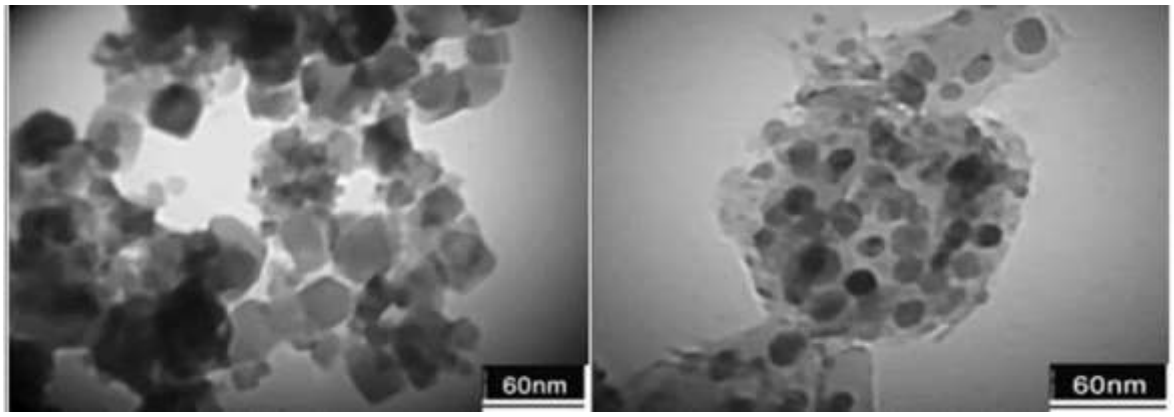

Figure 27 : TEM-F and FP NPs

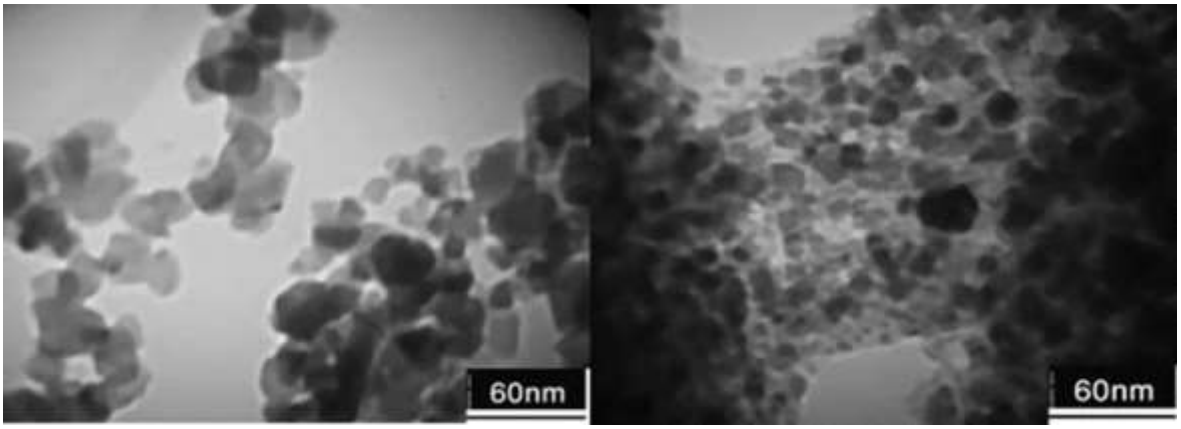

Figure 28 : TEM-HF and HFP NPs

FTIR Analysis:

FTIR analysis was also performed to identify the nature of the bonds in the synthesized nanoparticles and to finally confirm the presence of the elements (Mn, Zn, and Fe_3O_4). The result of this analysis is shown in Figures 29 and 30.

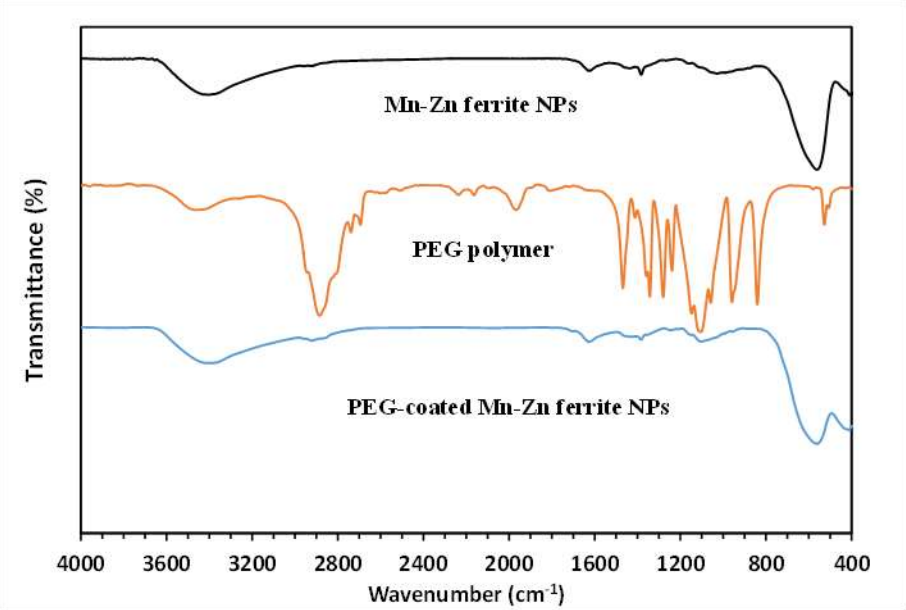

Figure 29 : Ferrites NPs and PEG coated Ferrite NPs

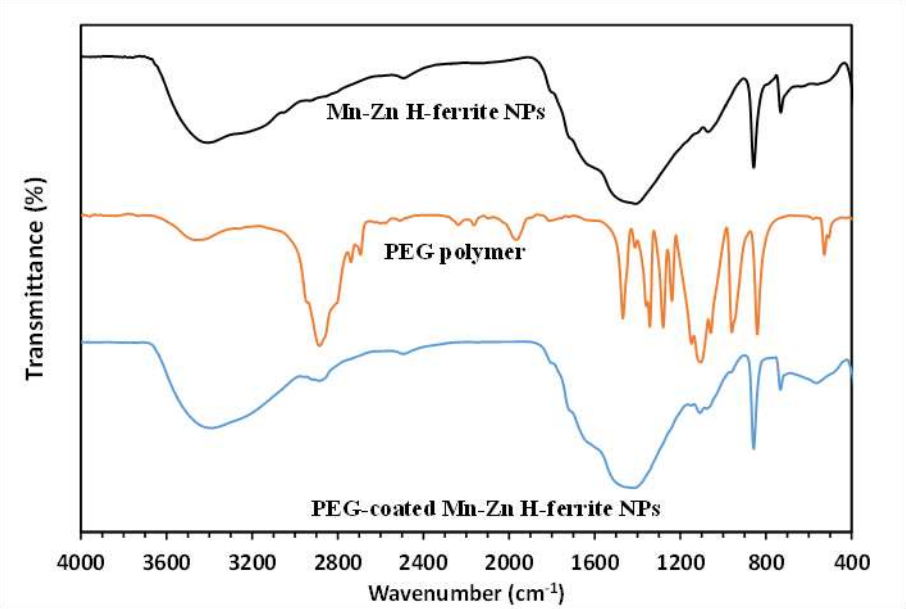

Figure 30 : Hierarchical Ferrite NPs and Hierarchical PEG coated Ferrite NPs

DLS analysis:

To verify the size distribution of the PEG coated nanoparticles, DLS analysis of the sample was performed. The result of this analysis is shown in Figures 31 and 32. As expected, the average size of the particles is about 100 nm, which is a confirmation of the thin PEG coating on the surface of the nanoparticles. Moreover, the single peak and the lack of width in the DLS diagram indicate a uniform distribution of the particle size.

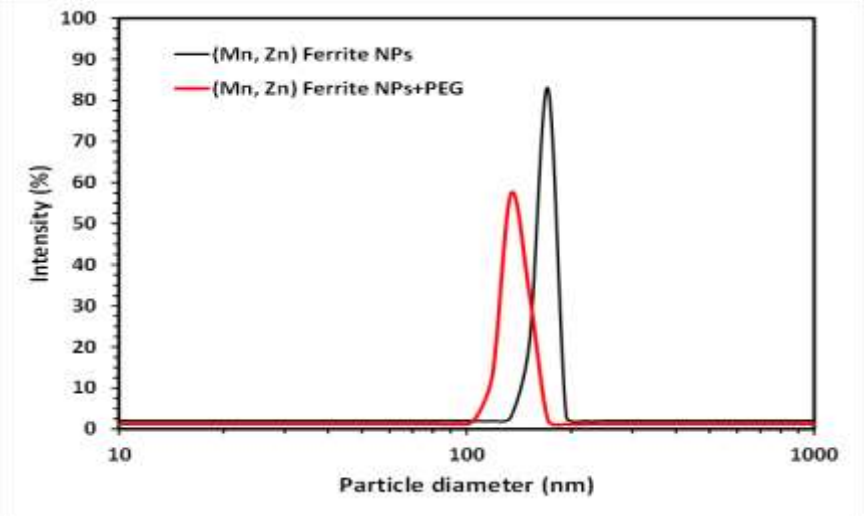

Figure 31 : Mn-Zn Ferrite NPs (black) and PEG coated Ferrite NPs (red)

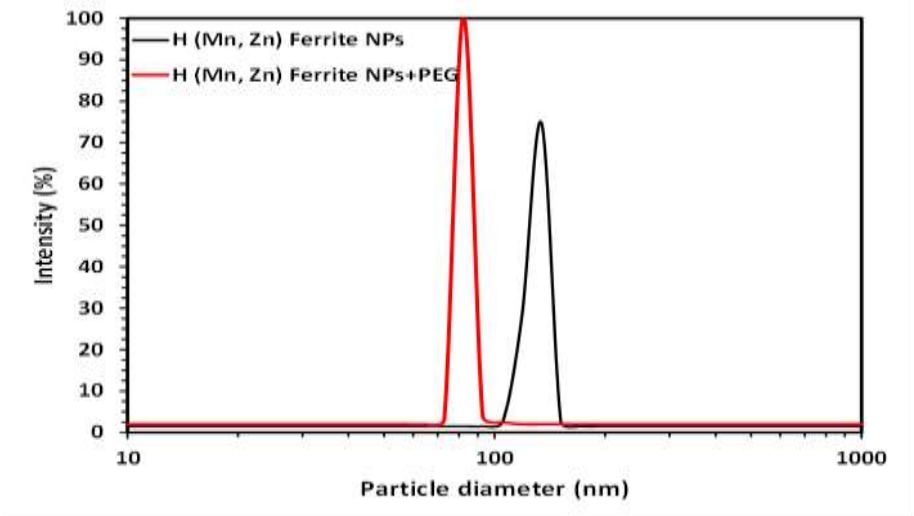

Figure 32 : Hierarchical Mn-Zn Ferrite NPs(black) and PEG coated Hierarchical Mn-Zn Ferrite NPs(red).

Zeta Analysis:

The zeta number indicates stability. If it is outside the range of +20 to -20, the particles are stable in the liquid environment. The more negative or positive the number, the stronger the surface charge, which means that the particles will not bind together. When the particles bind together, they become large and precipitate. Figures 33 and 34 show that the surface charge number for the particles is -50, indicating that the synthesized particles are stable in the colloid.

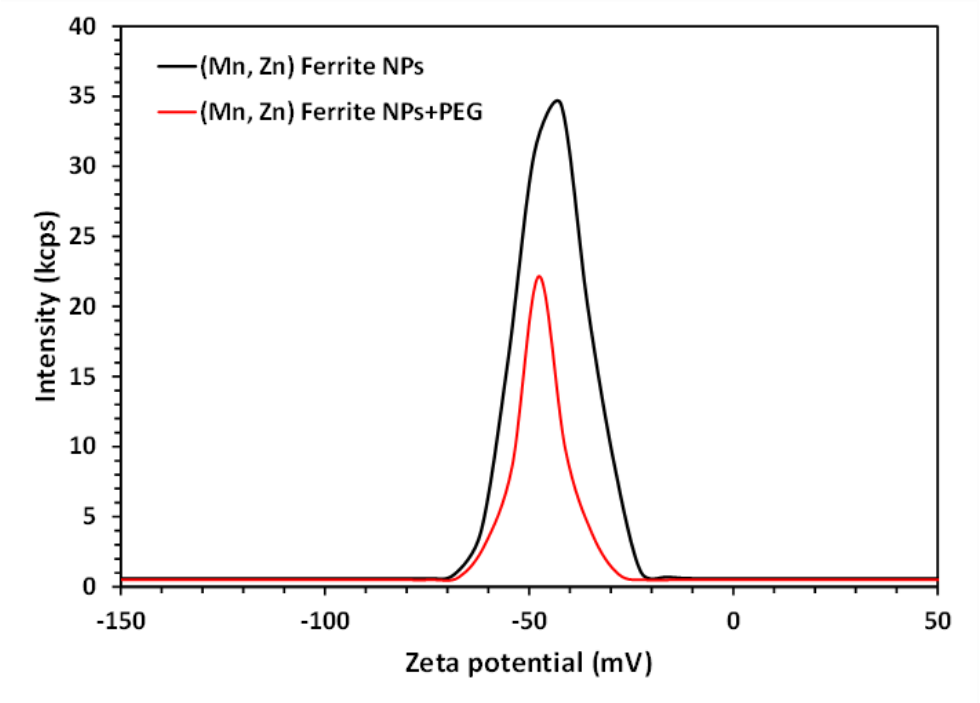

Figure 33 : Mn-Zn Ferrite NPs (black) and PEG coated Ferrite NPs (red)

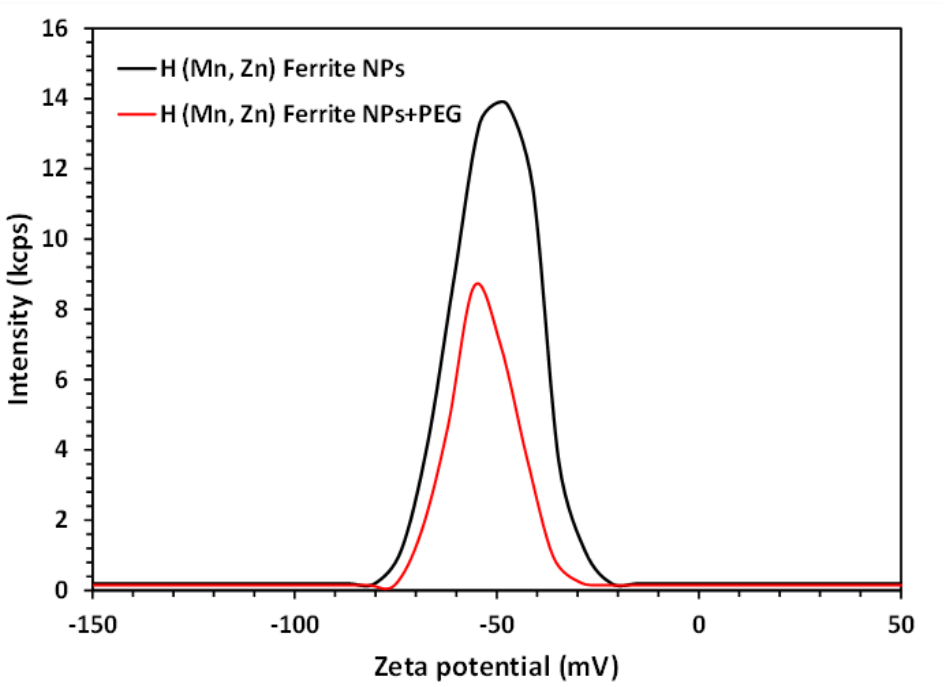

Figure 34: Hierarchical Mn-Zn Ferrite NPs(black) and PEG coated Hierarchical Mn-Zn Ferrite NPs(red).

ICP Analysis:

To accurately determine the percentage of the elements iron, manganese and zinc in the synthesized Mn-Zn ferrites NP and also in the hierarchical Mn-Zn ferrites NP with a pH of 1.30 and a time of 6 hours, the device ICP-MASS was used. The results of this analysis show the percentage of Fe, Mn and Zn in both the Mn-Zn ferrites NP and the hierarchical Mn-Zn ferrites NP. Figure 35 shows the exact percentage of each element.

Sample	Fe (wt. %)	Mn (wt. %)	Zn (wt. %)	Molar ratio (Fe/Mn+Zn)
F	65.1	18.3	16.6	1.99
HF	63.9	17.6	18.5	1.90

Figure 35: Exact percentage of the elements iron, manganese and zinc.

VSM Analysis:

A VSM analysis was performed to investigate the magnetic properties of zinc-manganese-ferrite samples synthesized at pH 1.30 and 10 for 6 hours with and without PEG coating. The results of this test can be seen in Figure 36. All of our products exhibit high saturation magnetization and are suitable for MRI applications. The hierarchical structure leads to a decrease in Ms, but it decreases from 66 to 59, which is still significant.

Finally, we can see that hierarchization has no bad effects on Ms. However, since PEG is a polymer coating, it is expected to decrease Ms. This effect is clearly seen in Figure 36 and also resulted in a decrease of Ms for coated ferrite to 53 and for hierarchical coated ferrite to 48. However, it is worth noting that coated ferrites still have a high MS. This implies that the presence of a PEG coating contributes to the stability of the colloid. In addition, other studies have shown that the presence of a PEG coating reduces toxic effects.

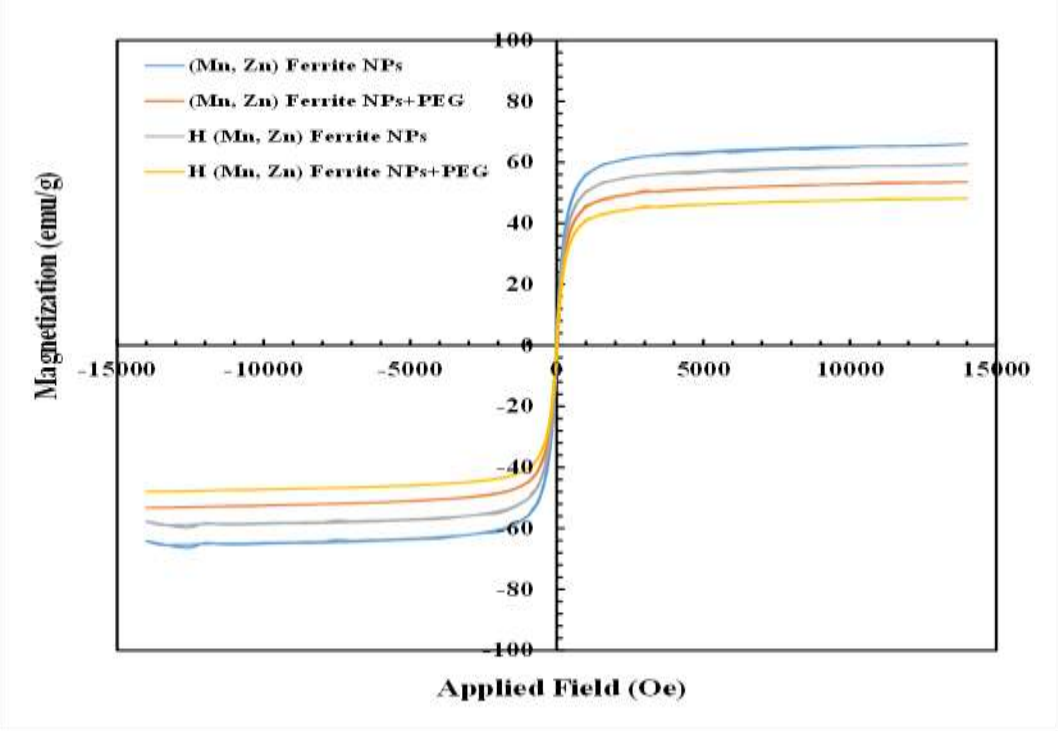

Figure 36 :The room-temperature magnetic hysteresis curves of the PEG-coated and uncoated Mn-Zn hierarchical ferrites NPS and normal NPS

Blood Analysis:

To investigate the effects of the in vitro combination of nanoparticles and blood samples, complete blood count (CBC) studies were performed on donor blood. Figure 37 shows CBC studies on 12 samples with three different concentrations.

Hemoglobin	Platelets	WBC	RBC	DENSITY	SAMPLE
15.4	267	7.26	5.62		MAIN SAMPLE
15.9	253	8.39	5.40	0.3	SAMPLE 1 F
16.2	245	8.08	5.52	0.3	SAMPLE 2 HF
16	250	8.47	5.48	0.3	SAMPLE 3 FP
16.1	247	8.54	5.48	0.3	SAMPLE 4 HFP
16.2	243	8.18	5.48	0.2	SAMPLE 5 F
16.1	251	8.14	5.42	0.2	SAMPLE 6 HF
16.2	256	8.44	5.51	0.2	SAMPLE 7 FP
16.1	246	8.41	5.47	0.2	SAMPLE 8 HFP
15.9	246	7.30	5.37	0.1	SAMPLE 9 F
15.8	237	7.52	5.39	0.1	SAMPLE 10 HP
15.7	257	7.58	5.32	0.1	SAMPLE 11 FP
15.9	250	7.49	5.38	0.1	SAMPLE 12HFP

Figure 37: Complete blood counts (CBC) studies (Normal Range: RBC: 4.5 – 6.1, WBC: 3.5 – 13, Platelets: 130 – 450, Hemoglobin: 13.2 – 18.5)

Blood Coagulation Analysis:

To investigate the effect of nanoparticles on clotting factors, a clotting assay was performed with donor blood. Figure 38 shows the exact number of clotting factors in 12 samples with three different concentrations.

aPTT	INR	PT activity	PT	DENSITY	SAMPLE
31.4	1.11	96	12.8		MAIN SAMPLE
29.5	1.12	95	12.9	0.3	SAMPLE 1 F
29.9	1.12	95	12.9	0.3	SAMPLE 2 HF
30.2	1.12	95	12.9	0.3	SAMPLE 3 FP
29.9	1.12	95	12.9	0.3	SAMPLE 4 HFP
30	1.13	94	13	0.2	SAMPLE 5 F
30	1.12	95	12.9	0.2	SAMPLE 6 HF
30.4	1.12	95	12.9	0.2	SAMPLE 7 FP
29.6	1.11	96	12.8	0.2	SAMPLE 8 HFP
30.1	1.12	95	12.9	0.1	SAMPLE 9 F
31.4	1.14	93	13.1	0.1	SAMPLE 10 HP
29.8	1.14	93	13.1	0.1	SAMPLE 11 FP
29.5	1.11	96	12.8	0.1	SAMPLE 12HFP

Figure 38 : In vitro blood coagulation studies (Normal Range: PT: 11.0 – 13.0 per sect, PT activity: %, INR: 0.9 – 1.15 mg Alb/gr cr, PTT: 24.0 – 36.0 per Sec)

MRI Test:

As we know, magnetic manganese ferrite nanoparticles have negative image resolution, and therefore the resulting image of the solution containing magnetic nanoparticles is dark compared to water or phosphate buffer solution. In fact, magnetic nanoparticles in the imaging process shorten the time taken by T_2. To investigate the effect of coating manganese zinc ferrite nanoparticles, in vitro MRI imaging was performed with pure manganese zinc ferrite nanoparticles and with peg-coated zinc manganese ferrite nanoparticles.

To compare the image resolution of pure manganese-zinc ferrite nanoparticles with hierarchical manganese-zinc ferrite, samples were prepared at three concentrations of 0.1, 0.2, and 0.3 mg/ml in distilled water solution and pH=10 and 1.30, respectively. The results of this test are shown in the figure 39. As expected, the nanoparticles in all 3 concentrations have the darkest image. In other words, the presence of these nanoparticles greatly increased the image resolution. Although the image resolution of the coated manganese

zinc ferrite nanoparticles is reduced due to the PEG coating, they still have relatively higher image resolution than the reference(water). These results are in good agreement with the VSM results.

In addition, MRI imaging was performed for all samples at concentrations greater than 0.3 and less than 0.1, but the results showed that all images were dark at concentrations greater than 0.3 and relatively bright at concentrations less than 0.1. Therefore, it can be said that the use of manganese-zinc-ferrite nanoparticles synthesized by hydrothermal method with PEG coating at a concentration of 0.1 to 0.3 mg/ml is suitable as contrast agents in MRI imaging.

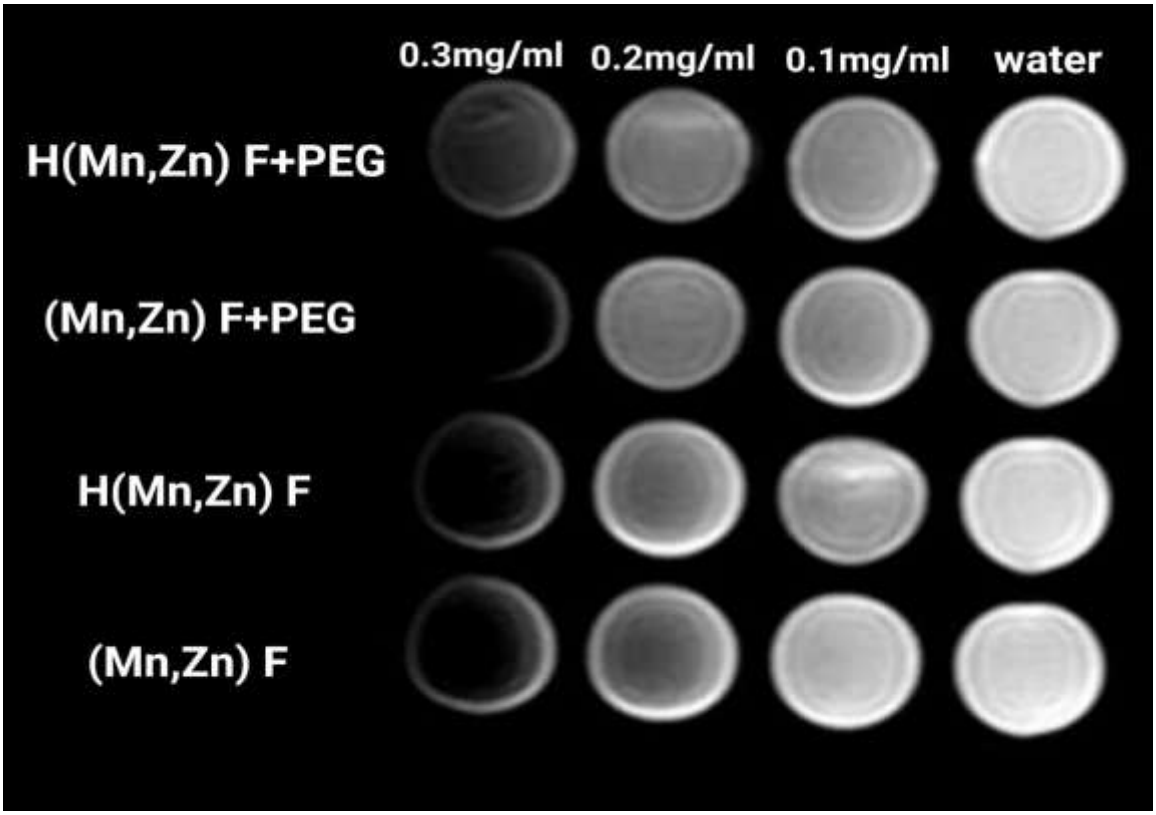

Figure 39: MRI images were acquired with Mn-Zn ferrite NPs, hierarchical Mn-Zn ferrite NPs, PEG coated Mn-Zn ferrite NPs and PEG coated hierarchical Mn-Zn ferrite NPs at concentrations of 0.1, 0.2, and 0.3 mg/ml in distilled water.

Chapter 4

Conclusion and Recommendations

Conclusion:

The novelty and main purpose of this research was to add materials to magnetic nanoparticles to change their structure to a hierarchical structure, which has never been used for MRI purposes. In addition, the hierarchical structure increases the specific surface area, which leads to positive results, especially for hyperthermia procedures.

In this research, the hydrothermal method was used to synthesize hierarchical manganese-zinc-ferrite nanoparticles, and then the synthesized nanoparticles were coated with PEG biocompatible polymer under optimal conditions. Finally, their magnetic properties and biocompatibility were evaluated. Overall, the following results were obtained in this research work:

1- Pure single-phase hierarchical Mn-Zn ferrite nanoparticles with a particle size of about 60 nm can be synthesized by a hydrothermal process at a pH of 1.30, a temperature of 160˚C, and a duration of 6 hours.

2-Biocompatible PEG polymer can be physically coated on Mn-Zn hierarchical ferrite nanoparticles synthesized by hydrothermal method.

3-The magnetic properties of the hierarchical Mn-Zn ferrite nanoparticles synthesized by the hydrothermal method have improved compared with Fe_3O_4 nanoparticles, and the Ms value has decreased from 66 to 59. Although the application of the biocompatible coating PEG has led to a decrease in the Ms value of the hierarchical Mn-Zn nanoparticles, it is still higher than that of Fe_3O_4.

4- Complete blood cell count (CBC) and blood clotting factor studies under laboratory conditions have shown that hierarchical Mn-Zn nanoparticles have no negative effects on blood factors.

5. The hierarchical Mn-Zn ferrite nanoparticles synthesized and coated in this study at concentrations between 0.1 and 0.3 mg/mmol can be used as MRI contrast agents.

Recommendations:

1-Use of other biocompatible coatings such as chitosan and silica to modify the surface of nanoparticles.

2-A cytotoxicity assay using a cell line is proposed to further investigate the biocompatibility of nanoparticles.

3-MRI imaging in vivo using zinc-manganese-ferrite nanoparticles synthesized by a hydrothermal method.

4-These nanoparticles may be a suitable candidate for the hyperthermia method to treat all types of cancer

5- To make Mn-Zn ferrites acceptable for use in electrical and agricultural applications, they can be doped with other metals such as cobalt, zinc, and magnesium to improve their electrical and magnetic properties.

6- Perform the BET test to investigate nanoparticle applications where the specific surface area is effective, such as drug delivery systems.

References

(n.d.). Retrieved from Phi4tech: https://www.phi4tech.com/nanomaterials/

IMA: Magnet factory and magnetic applications. (2018). Retrieved from https://imamagnets.com/

Magnetic Hysteresis. (2022). Retrieved from Electromagnetism : https://www.electronics-tutorials.ws/

(2004, Dec 14). Retrieved from AZO NANO: https://www.azonano.com/article.aspx?ArticleID=1079

(2016, April 12). Retrieved from bestknowledgesite: http://bestknowledgesite.weebly.com/

A.C.F.M. Costa. (2008). Ni–Zn–Sm nanopowder ferrites: Morphological aspects and magnetic properties. *Magnetism and Magnetic Materials 320*, 742–749.

A.P.A.Faiyas. (2010). Dependence of pH and surfactant effect in the synthesis of magnetite (Fe3O4) nanoparticles and its properties. *Magnetism and Magnetic Materials*, 400-404.

Abdel-Mohsen Onsy Mohamed. (2018). Magnetic Properties of Soils. *Fundamentals of Geoenvironmental Engineering*.

Aditya Chauhan. (2012). Magnetic material selection using multiple attribute decision making approach. *Materials and Design 36*, 1-5.

Ananya Renuka Balakrishna. (2020). A tool to predict coercivity in magnetic materials. *Creative Commons Attribution 4.0 International*.

anurag652. (2021, Sep 21). *Magnetization and Magnetic Intensity*. Retrieved from https://www.geeksforgeeks.org/

Ashish Avasthi. (2020). Magnetic Nanoparticles as MRI Contrast Agents. *Springer Link*.

Awadallah, A. (2015, July). *Researchgate*. Retrieved from https://www.researchgate.net/

B. Skołyszewska. (2003). Preparation and magnetic properties. *science direct*, 290–294.

Bashar Issa. (2013). Magnetic Nanoparticles: Surface Effects and Properties Related to Biomedicine Applications. *International Journal of Molecular Sciences*.

Bin Cai. (2015). Bioinspired Formation of 3D Hierarchical CoFe2O4 Porous Microspheres for Magnetic-Controlled Drug Release. *ACS Appl Mater Interfaces*.

Brain MRI. (2022). Retrieved from health/diagnostics/-brain-mri: https://my.clevelandclinic.org

British Heart Foundation. (2016, May 16). Retrieved from https://www.bhf.org.uk

C.Pullar, R. (2012). Hexagonal ferrites: A review of the synthesis, properties and applications of hexaferrite ceramics. *Materials Science*, 1191-1334.

Christo B. Tsvetanov. (2012). High-Molecular-Weight Poly(ethylene oxide). *Elsevier*.

Clare, S. (1997). *Functional MRI : Methods and Applications.* Nottingham: University of Nottingham.

D.O'Hare. (2001). Hydrothermal Synthesis. In *Encyclopedia of Materials: Science and Technology (Second Edition)* (pp. 3989-3992).

Daliya S.Mathew. (2007). An overview of the structure and magnetism of spinel ferrite nanoparticles and their synthesis in microemulsions. *Chemical Engineering*, 51-65.

Dmitry Bokov. (2021). Nanomaterial by Sol-Gel Method: Synthesis and Application. *Advances in Materials Science and Engineering*.

E. Spain. (2014). Review of Physical Principles of Sensing and Types. *Elsevier Ltd.*

E. Spain. (2014). Sensor Materials, Technologies and Applications. *Comprehensive Materials Processing*.

Ehsan Kianfar. (2021). Nanomaterial by Sol-Gel Method: Synthesis and Application. *Advances in Materials Science and Engineering*.

FDA Drug Safety Communication: FDA warns that gadolinium-based contrast agents (GBCAs) are retained in the body; requires new class warnings. (2017, 05 22). Retrieved from U.S. FOOD & DRUG ADMINISTRATION: https://www.fda.gov/drugs/drug-safety-and-availability/fda-drug-safety-communication-fda-warns-gadolinium-based-contrast-agents-gbcas-are-retained-body

Gayathri Thirumalraj. (2015). Gadolinium Oxide Nanoparticles for Magnetic Resonance Imaging and Cancer Theranostics. *Bionanoscience*.

Giuliana Gorrasi. (2015). Mechanical milling as a technology to produce structural and functional bio-nanocomposites†. *Green Chemistry*.

Guadalupe Gabriel Flores-Rojas. (2022). Magnetic Nanoparticles for Medical Applications:Updated Review. *MDPI*.

H.-J. Qiu a. (2015). Hierarchical nanoporous metal/metal-oxide composite by dealloying metallic glass for high-performance energy storage. *Corrosion Science*, 196-202.

Han-Wen Cheng. (2016). Assessment of aggregative growth of MnZn ferrite nanoparticles. *royal society of chemistry*.

Humaira Anwar. (2012). Effect of Sintering Temperature on Structural, Electrical and Dielectric Parameters of Mn-Zn Nano Ferrites. *Key Engineering Materials Vols 510-511*, 163-170.

IbrahimKhan. (2019). Nanoparticles: Properties, applications and toxicities. 908-931.

IbrahimKhan. (2019). Nanoparticles: Properties, applications and toxicities. *Arabian Journal of Chemistry*, 908-931.

J. Hemapriya. (2019). *Chitosan and Its Biomedical Applications.* Jenny Stanford .

Jessica Wahsner. (2018). Chemistry of MRI Contrast Agents: Current Challenges and New Frontiers. *Chemical reviews*.

JinAh Hwang. (2020). Structural and Magnetic Properties of NiZn Ferrite Nanoparticles Synthesized by a Thermal Decomposition Method. *applied science*.

Jinkwon Kim. (2008). Self-Assembly and Photopolymerization of Diacetylene Molecules on Surface of Magnetite Nanoparticles.

K.Petcharoen. (2012). Synthesis and characterization of magnetite nanoparticles via the chemical co-precipitation method. *Materials Science and Engineering B*, 421-427.

Karin H.Müller. (2014). The effect of particle agglomeration on the formation of a surface-connected compartment induced by hydroxyapatite nanoparticles in human monocyte-derived macrophages. *Biomaterials*, 1074-1088.

kianfar, E. (2021). Magnetic Nanoparticles in Targeted Drug Delivery: a Review. *Superconductivity and Novel Magnetism volume*, 1709–1735.

Kirchmayr1, H. R. (1996). Permanent magnets and hard magnetic materials. *Applied Physics*.

Kohnert, R. L. (1993). Retrieved from polymer.htm: http://chemiris.chem.binghamton.edu/

Kullaiah Byrappa. (2001). History of Hydrothermal Technology. 53-81.

Kumhar, V. (2021, April 1). *antsLAB*. Retrieved from Global Manufacturer and Distributor of Ceramic Crucibles and Labwares: https://www.antslab.in/

Lakshita Phor. (2019, Dec). Retrieved from SN Applied Sciences: https://www.researchgate.net/

(2022). *Magnetic Resonance Imaging (MRI).* Bethesda: National Institute of Biomedical Imaging and Bioengineering. Retrieved from https://www.nibib.nih.gov/

Manjeet S.Dahiya. (2018). 31 - Metal–ferrite nanocomposites for targeted drug delivery. *Applications of Nanocomposite Materials in Drug Delivery*, 737-760.

Mansfield, P. (2003, Dec 8). SNAP-SHOT MRI.

MarthaPardavi-Horvath. (2000). Microwave applications of soft ferrites. *Magnetism and Magnetic Materials*, 171-183.

Mayor, S. (2003). Nobel prize in medicine awarded to MRI pioneers. *NIH*.

MEDICOVER. (2022). Retrieved from Whole body MRI examination: https://medicover.hu/

MGA. (2012). Retrieved from http://magnetga.ir/

Michael A. Ibrahim. (2022). Gadolinium Magnetic Resonance Imaging. *NIH*.

Mills, A. A. (2010). The Lodestone: History, Physics, and. *Annals of Science*.

Moskowitz, B. M. (1991, June 5-8). *College of Science and Engineering*. Retrieved from Universitu Of Minnesota: https://cse.umn.edu/

N. Modaresi. (2019). Magnetic properties of ZnxFe3-xO4 nanoparticles: A competition between the effects of size and Zn doping level. *Magnetism and Magnetic Materials*.

N.M. Deraz∗. (2012). Structural, morphological and magnetic properties of nano-crystalline zinc substituted cobalt ferrite system. *Analytical and Applied Pyrolysis 94*, 41-47.

national MAGLAB. (2012-2022). Retrieved from Magnet Academy: https://nationalmaglab.org/

Oscar Oehlsen. (2022). Approaches on Ferrofluid Synthesis and Applications: Current Status and Future Perspectives. *acsodf*, 3134-3150.

P. Majewski. (2009). *Particulate systems in Nano and Biotechnologies.*

PHAM THANH PHONG. (2015). Studies of the Magnetic Properties and Specific Absorption of Mn0.3Zn0.7Fe2O4 Nanoparticles. *ELECTRONIC MATERIALS, Vol. 44, No. 1,*.

Preeti Thakur. ((2020)). A review on MnZn ferrites: Synthesis, characterization and applications. *Ceramics International 46*, 15740–15763.

R.C.O'Handleya. (2003). Magnetic Materials. *Encyclopedia of Physical Science and Technology (Third Edition)*, 919-944.

RadilogyInfo.org. (2020, June 15). Retrieved from https://www.radiologyinfo.org/en/info/bodymr.

Radiological Society of North America, I. (. (2022). *Spine MRI*. Retrieved from en/info/spinemr: https://www.radiologyinfo.org

Raymond Damadian. (1974). Human Tumors Detected by Nuclear Magnetic Resonance.

Rinck, P. A. (2008). A short history of magnetic resonance imaging. *European Magnetic Resonance Forum Fundation*. Retrieved from https://www.spectroscopyeurope.com/

RoshaidaArbain. (2011). Preparation of iron oxide nanoparticles by mechanical milling. *Minerals Engineering*, 1-9.

Rouhollah Khodadust. (2012). Synthesis optimization and characterization of chitosan-coated iron oxide nanoparticles produced for biomedical applications. *Gozde UNSOY*.

royaniran. (2020, Dec 8). Retrieved from https://royaniran.com/

S. Palagummi,. (2016). Magnetic levitation and its application for low frequency vibration energy harvesting. *Structural Health Monitoring (SHM) in Aerospace Structures*. Retrieved from https://www.britannica.com/

S.A.V. Prasad. (2018). Synthesis of MFe2O4 (M=Mg2+, Zn2+, Mn2+). *Ceramics International*.

S.F. Mansour. (2017). Improvement on the magnetic and dielectric behavior of hard/soft ferrite. *Molecular Structure*.

S.Geller. (2002). The crystal structure and ferrimagnetism of yttrium-iron garnet, Y3Fe2(FeO4)3. *Physics and Chemistry of Solids*.

Saikat Chaudhuri. (2021). Green synthetic approaches for medium ring–sized heterocycles of biological and pharmaceutical interest. *Green and Sustainable Chemistry*, 617-653.

Santosh K. Gupta. (2021). A review on molten salt synthesis of metal oxide nanomaterials:. *Progress in Materials Science*.

Sapna. (2018). Shape-controlled synthesis of superparamagnetic ZnFe2O4 hierarchical structures and their comparative structural, optical and magnetic properties. *Ceramics International*.

Schenck, J. F. (2003). *Magnetic Resonance in Medicine.* Encyclopedia of Physical Science and Technology (Third Edition).

Seipati Rosemary Mokhosi . (2022). Advances in the Synthesis and Application of Magnetic Ferrite Nanoparticles for Cancer Therapy. *MDPI*.

SemaÇalış. (2019). Nanopharmaceuticals as Drug-Delivery Systems. *Nanocarriers for Drug Delivery*, 133-154.

Sophie Laurent. (2008). Magnetic Iron Oxide Nanoparticles: Synthesis, Stabilization, Vectorization, Physicochemical Characterizations, and Biological Applications. *Chem. Rev*, 2064–2110.

SPIN PHYSICS. (2020). Retrieved from The Basics of MRI (CHAPTER 3): https://www.cis.rit.edu/

Stark, W. J. (2011). Nanoparticles in Biological Systems. *Angewandte*, 1242 – 1258.

Sugimoto, M. (1999). The Past, Present, and Future of Ferrites. *american ceramic society*, 269-80.

Tao Sun. (2011). Synthesis and Characterization of Nanocrystalline Zinc Manganese Ferrite. *american ceramic society 94*, 1490–1495.

the physics classroom. (n.d.). Retrieved from https://www.physicsclassroom.com/

Thomas Dippong. (2021). Recent Advances in Synthesis and Applications of MFe2O4. *MDPI*.

Vishnu D.Rajput. (2021). Nanomaterials for Soil Remediation. 65-85.

WOLFRAM. (2022). Retrieved from https://reference.wolfram.com

YangyangLong. (2014). Modeling and optimization of the molten salt cleaning process. *Cleaner Production*, 243-251.

Yao-Ming Hao,. (2012). Structural, optical, and magnetic studies of manganese-doped zinc oxide hierarchical microspheres by self-assembly of nanoparticles. *a SpringerOpen*.

Zuzanna Bielan. (2021). Application of Spinel and Hexagonal Ferrites in Heterogeneous Photocatalysis. *MDPI*.